

Fall 12-2020

Experimental Analysis of Heat Generation in Carbon

Mounisha Ganesan
Embry-Riddle Aeronautical University

Follow this and additional works at: <https://commons.erau.edu/edt>



Part of the [Structures and Materials Commons](#)

Scholarly Commons Citation

Ganesan, Mounisha, "Experimental Analysis of Heat Generation in Carbon" (2020). *Doctoral Dissertations and Master's Theses*. 554.

<https://commons.erau.edu/edt/554>

This Thesis - Open Access is brought to you for free and open access by Scholarly Commons. It has been accepted for inclusion in Doctoral Dissertations and Master's Theses by an authorized administrator of Scholarly Commons. For more information, please contact commons@erau.edu.

EXPERIMENTAL ANALYSIS OF HEAT GENERATION IN CARBON
NANOTUBES

By

Mounisha Ganesan

A Thesis Submitted to the Faculty of Embry-Riddle Aeronautical University
In Partial Fulfillment of the Requirements for the Degree of
Master of Science in Aerospace Engineering

December 2020

Embry-Riddle Aeronautical University

Daytona Beach, Florida

EXPERIMENTAL ANALYSIS OF HEAT GENERATION IN CARBON NANOTUBES

By

Mounisha Ganesan

This thesis was prepared under the direction of the candidate's Thesis Committee Chairs, Dr. Virginie Rollin and Dr. Daewon Kim, Department of Aerospace Engineering, and has been approved by the members of the Thesis Committee. It was submitted to the Office of the Senior Vice President for Academic Affairs and Provost, and was accepted in the partial fulfillment of the requirements for the Degree of Master of Science in Aerospace Engineering.

THESIS COMMITTEE

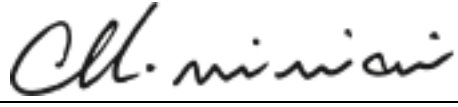
Chairman, Dr. Virginie Rollin

Co-Chairman, Dr. Daewon Kim

Member, Dr. Foram Madiyar

Graduate Program Coordinator,
Dr. Marwan Al-Haik

Date



Dean of the College of Engineering,
Dr. Maj Mirmirani

Date

Associate Provost of Academic Support,
Dr. Christopher Grant

Date

ACKNOWLEDGEMENTS

I would like to dedicate this thesis to my family. Firstly, I would like to thank my parents L. Ganesan, V. Karpagam, my sister G.Srinidhi, and my friend Pralay for their constant support and encouragement throughout my study at Embry-Riddle Aeronautical University.

I am extremely grateful to my faculty advisor Dr. Marwan Al-Haik for providing me the opportunity in carrying out this dissertation work.

I would like to express my deep and sincere gratitude to my research advisors, Dr. Virginie Rollin and Dr. Daewon Kim, for accepting me to conduct research and providing invaluable support and guidance throughout this research.

I wish to extend my hearty thanks to my thesis committee member Dr. Foram Madiyar for her endless support in sharing her expertise, guidance and continuous encouragement throughout the thesis.

I would like to thank my entire thesis committee for their dedication and enthusiasm that motivated me to strive for excellence and bring the best out of me. I would like to thank their friendliness, empathy and showing support and care by every means that is possible.

I would like to extend my hearty thanks to Mr. Michael S. Potash for his valuable insights and discussions on thermal devices and circuits. I am extremely grateful to Dr. David Sypeck for providing experimentation help and support as needed.

I would like to thank my lab colleagues Sahil Ghate and John Veracka, for their hands-on help and support throughout the experimentation process.

ABSTRACT

The purpose of this research is to study a novel non-covalent functionalization technique of single-walled carbon nanotubes (SWCNTs) and to examine the feasibility of using carbon nanotube films as thin film heaters. We developed a unique methodology to synthesize a well dispersed, environmentally friendly solution of CNTs that could be easily spin coated as well as spray coated on different substrates based on the application. Using the produced solutions, thin films of SWCNTs were fabricated on a glass substrate. Two sets of experiments were conducted to study the influence of polyaromatic moiety and the pH on the electro thermal characteristics of the fabricated film heater. Comparative tests were done on the carbon nanotube-based film heater samples to study the film's resistance and heat generated with the application of input power. It was found that samples resistance varied significantly based on the amount of polyaromatic moiety added to the CNTs and the fabricated films did not show any linear trend when comparative test was made based on pH. To the best of our knowledge, this is the first report analyzing the influence of polyaromatic moiety and the pH on the resistance and heat characteristics of the fabricated film heater. We present experimental results showing that the developed approach and the modified CNT material could be a promising alternative for heating applications such as deicing and defrosting. Further, this study also discusses the limitations and improvements needed in experimentation process that could yield high performance CNT based heaters. The fabricated CNT films show fast heating and cooling rate at a low driving voltage. The results provided could be a useful approach for the engineering of highly flexible transparent CNT-based heaters.

TABLE OF CONTENTS

ACKNOWLEDGEMENTS.....	ii
ABSTRACT.....	iii
LIST OF FIGURES.....	vi
LIST OF TABLES.....	ix
NOMENCLATURE.....	x
1. Introduction.....	1
1.1. Structure and Properties of Carbon Nanotubes.....	2
1.1.1. Types of CNT.....	3
1.1.1.1. Single-Walled Carbon Nanotubes.....	3
1.1.1.2. Multi-Walled Carbon Nanotubes.....	4
1.1.2. Properties of CNTs.....	5
1.2. Current Applications of Carbon Nanotubes.....	7
1.3. Aim of this Research.....	8
1.4. Need for this Research.....	9
1.4.1. Limitations of Conventional Materials.....	9
1.4.2. Demand in Aircraft and Automotive Applications.....	10
1.5. Motivation of Research.....	12
1.6. Importance of Research.....	13
1.6.1. Objective.....	13
1.6.2. Outline of Chapters.....	14
2. Research Methodology.....	15
2.1. Research Approach.....	15
2.1.1. Synthesis of SWCNT Solution.....	15
2.1.1.1. Functionalization Methods.....	16
2.1.1.1.1. Covalent Functionalization.....	17
2.1.1.1.2. Non-Covalent Functionalization.....	18
2.1.1.2. Chemical Materials Used.....	19
2.1.1.3. Solution Synthesis Methodology.....	19
2.1.1.4. Experiments Performed.....	22
2.1.2. Fabrication of SWCNT Films.....	24
2.1.2.1. Substrate Preparation.....	24
2.1.2.2. Spin Coating.....	26
2.1.2.3. Electrode Application.....	29
2.2. Characteristics of Fabricated Film Heater.....	29
2.2.1. Heating Mechanisms.....	31
2.2.1.1. Concept of Joule Heating.....	31
2.3. Summary.....	33

3. Testing and Results.....	34
3.1. Testing Methods.....	34
3.1.1. Resistance testing.....	34
3.1.1.1. Resistance test results.....	35
3.1.2. Apparatus and Materials.....	42
3.1.2.1. Electrothermal Performance Testing.....	42
3.1.2.2. Electrothermal Test Results.....	44
3.1.2.3. Repeatability Testing.....	49
3.1.3. Transmittance Testing.....	51
3.1.3.1. Transmittance Testing Results.....	51
3.1.4. Sample Characterization.....	53
3.2. Summary.....	54
4. Discussion, Conclusions, and Recommendations	55
4.1. Discussion.....	55
4.2. Conclusions.....	56
4.3. Recommendations and Future Work.....	58
4.4. Summary.....	60
REFERENCES.....	61

LIST OF FIGURES

Figure	Page
1.1 Schematic view of graphene rolled up to CNT (Zuo, 2018).....	2
1.2 Classification of CNTs are armchair, chiral, and zigzag CNTs (J. Sisto et al., 2016).....	4
1.3 a) Schematic of multi-walled carbon nanotubes, b) Scanning electron microscopic image of raw multi-walled carbon nanotubes (Chen, 2016).....	5
1.4 Application of CNTs in composites, sensors, energy storage devices, biomedical and thermal devices.....	8
1.5 Icing on the windshield, leading-edge, and propeller blades (Briefing, 2020)...	10
1.6 Aircraft icing accidents from 1981-2009 (Duchon, 2010).....	11
2.1 Representation of different methods of functionalization of CNTs (Karimi et al., 2015).....	17
2.2 Non covalent functionalization of CNTs using polyaromatic moiety pyrene derivative and acid (Preparation and Properties of Carbon Nanotube-Based Inks, 2014).....	20
2.3 Solutions of experiment 1 and experiment 2 a) before centrifuge, b) after centrifuge.....	22
2.4 Fabricated solutions of experiment 1 and experiment 2.....	23
2.5 Preparation of the substrate before spin coating a) Cleaning of slides in DI water, b) Cleaning of slides with isopropyl alcohol and rinsing in DI water, c) Plasma applicator (BD-20AC Laboratory Corona Treater, 2020), d) Treating of cleaned slides with the application of plasma.....	25
2.6 Schematics of steps involved in spin coating from application of solution to creation of thin films (Mishra et al., 2019).....	26
2.7 Schematic of fabrication of film heater a) Clean plasma treated glass slides, b) CNT spin coated glass substrate, c) Application of silver pain on the fabricated film.....	29
2.8 Spin coated samples of fabricated film heater.....	30

Figure	Page
2.9 Model of carbon nanotube film heater and representation of heat generated due to the presence of network of CNTs.....	32
3.1 Resistance of CNT film samples of experiment 1 with silver paint as electrode.....	36
3.2 Resistance of CNT film samples of experiment 2 with silver paint as the electrode.....	36
3.3 Resistance test results of experiments 1 and 2 with silver epoxy as electrode...	41
3.4 Block diagram representing the process involved in electrothermal testing (top), Electrothermal test setup in the laboratory (bottom).....	43
3.5 IR camera images of heat generation in fabricated film heater, a) Film heater before application of voltage, b) Gradual heat generation after application of voltage, c) Uniform distribution of heat over the entire film, d) Film heater after the voltage was turned off.....	44
3.6 Temperature increase profile for CNT films of a) experiment 1 and b) experiment 2 at applied voltage of 20V.....	45
3.7 a) Maximum temperature increase for samples 1 of experiment 1 and experiment 2, b) Maximum temperature increase dependency on film resistance.....	47
3.8 Temperature derivative curves for the samples of experiment 1 and 2 plotted over time.....	48
3.9 Current, voltage and power characteristics of the CNT film heater, a) Change of current for incremental voltage in steps of 5 from 0 to 20 V, b) Power of the heater for incremental voltage in steps of 2.22V from 0 to 20 V.....	49
3.10 Temperature increase profiles for experiments 1 and 2 at an applied voltage of 20 V repeated for 3 trials on the same sample. a) Experiment 1-A, b) Experiment 1-B, c) Experiment 1-C, d) Experiment 2-A, e) Experiment 2-B, f) Experiment 2-C.....	50
3.11 Transmittance spectra of fabricated CNT films in the visible light spectra. Transmittance of a) experiment set 1 and b) experiment 2 taken at room temperature.....	52

Figure	Page
3.12 SEM image of film heater containing 3 layers of spin coated CNTs taken at different spots. a) Morphology of CNTs deposited on the film at 30000x magnification, b) Length of CNTs measured in SEM at 30000x magnification.....	53

LIST OF TABLES

Table	Page
2.1 Synthesized solution, pH, and amount of compounds in experiment 1.....	23
2.2 Synthesized solutions, pH and amount of compounds in experiment 2.....	24
2.3 Samples produces using different spin speed combination.....	28
3.1 Quantity of samples prepared for experimental sets 1 and 2 using silver paint and silver epoxy as electrode.....	34
3.2 Resistance characteristics of CNT film samples of experiment 1 with silver paint as the electrode.....	39
3.3 Resistance characteristics of CNT film samples of experiment 2 with silver paint as the electrode.....	40
3.4 Tabulation of maximum temperature increase attained by each sample and their response time.....	46

NOMENCLATURE

CNT	-	Carbon nanotubes
SWCNT	-	Single-walled carbon nanotubes
MWCNT	-	Multi-walled carbon nanotubes
PBA	-	1-Pyrenebutyric acid
NH ₄ OH	-	Ammonium hydroxide
OLED	-	Organic light emitting diode
DNA	-	Deoxyribonucleic acid
ITO	-	Indium tin oxide
SEM	-	Scanning electron microscope
rpm	-	Revolution per minute
DI	-	Deionized water
IR	-	Infrared camera
DC	-	Direct current
°C	-	Degree centigrade
KΩ	-	Kilo Ohm
cm	-	centimeter
μm	-	micrometer
nm	-	nanometer
m	-	meter
W	-	Watt
K	-	Kelvin
H	-	Heat generated

I	-	Current
P	-	Power
V	-	Voltage
t	-	Time
ΔT	-	Temperature difference

1. Introduction

Carbon is known to be the most versatile element on earth. Modifying the arrangement of carbon atoms leads to new forms of carbon, such as graphite and diamond. In 1980, graphite, diamond, and amorphous carbon were the only known forms of carbon structures. Carbon is a long-studied element, but that does not mean there is nothing more to discover. In 1985, a surprising unintended experiment led to the discovery of a whole new class of molecules purely made of carbon called the Fullerenes. The synthesis of buckminsterfullerene C_{60} led to the discovery of carbon nanotubes (Aqel et al., 2012).

In 1991, Sumo Iijima first synthesized multiwalled CNTs (MWCNTs) in an arc-discharge method and observed that on each tube, carbon atoms are arranged in a helical fashion about the needle axis (Iijima, 1991). These nanotubes were found to have two or more layers (Multi-walled CNTs), and their outer diameter ranged from about 2nm to 100 nm (Amenta & Aschberger, 2015). After two years, in 1993, Iijima, Ichihashi, and Bethune produced single-walled CNTs using a metal catalyst in the arc-discharge method (E.N.Ganesh, 2013).

Riding on the excitement created by the discovery of new carbon allotropes, carbon nanotubes (CNT) inspired several researchers to study their various aspects and properties. Amongst all carbon nanomaterials, carbon nanotubes generated a great deal of interest amongst scientists, engineers, and researchers due to their exceptional combination of properties. It is the structure, topology, and size of the CNTs that makes their properties stand unique compared to planar graphite structure (Ajayan & Zhou, 2001).

1.1. Structure and Properties of Carbon Nanotubes

CNTs are cylindrical nano molecules that can be visualized as a layer of graphene rolled up to give a cylindrical structure with carbon atoms 0.14 nm apart at each apex. A schematic representation of the CNT is given in Figure 1.1. CNTs are sp^2 hybridized carbon atoms like fullerenes and are often known as tubular fullerenes (Khalid Saeed, 2013). The diameter of carbon nanotubes is less than 100 nm nanometers, and their length ranges from a few hundred nanometers to centimeters, yielding an unparalleled length/diameter aspect ratio exceeding 10^7 (Jorio et al., 2008). The diameter and length could be selectively produced based on growth and treatment processes that yield CNTs of diameter from 2 to 100 nm and length ranging from 1 to 15 μm (Prasek et al., 2011).

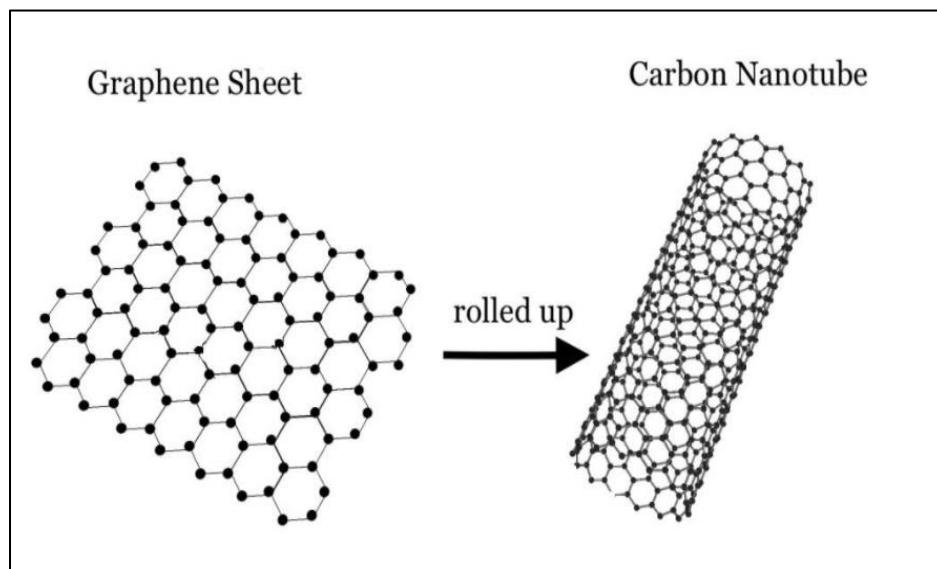


Figure 1.1 Schematic view of graphene rolled up to CNT (Zuo, 2018)

1.1.1. Types of CNT

CNTs can be mainly classified as:

1. Single-walled carbon nanotubes (SWCNTs)
2. Multi-walled carbon nanotubes (MWCNTs)

1.1.1.1. Single-Walled Carbon Nanotubes

When a CNT is formed by rolling a single layer of carbon atoms (Graphene), it is called single-walled CNTs (Parijat Pandey, 2016). The diameter of SWCNTs ranges between 0.7 nm and 10 nm, however, it is mostly observed to be less than 2 nm (R. Saito, 1998). Often these nanotubes are one-dimensional nanostructures. SWCNTs can be further categorized based on their symmetry. The primary symmetry classification of CNTs is achiral and chiral, where achiral meaning the CNT and its mirror image have an identical structure and are superimposable (R. Saito, 1998). There are two types of achiral SWCNTs, namely armchair and zigzag nanotubes (R. Saito, 1998). Chiral nanotubes exhibit a spiral symmetry whose mirror image cannot be superimposed (R. Saito, 1998). The three possible types of CNTs, namely armchair, zigzag, and chiral, arise depending on the choice of the rolling axis relative to the hexagonal network of the graphene sheet (Saifuddin et al., 2012). *Figure 1.2* represents the configuration of armchair, zigzag, and chiral CNTs (J. Sisto et al., 2016).

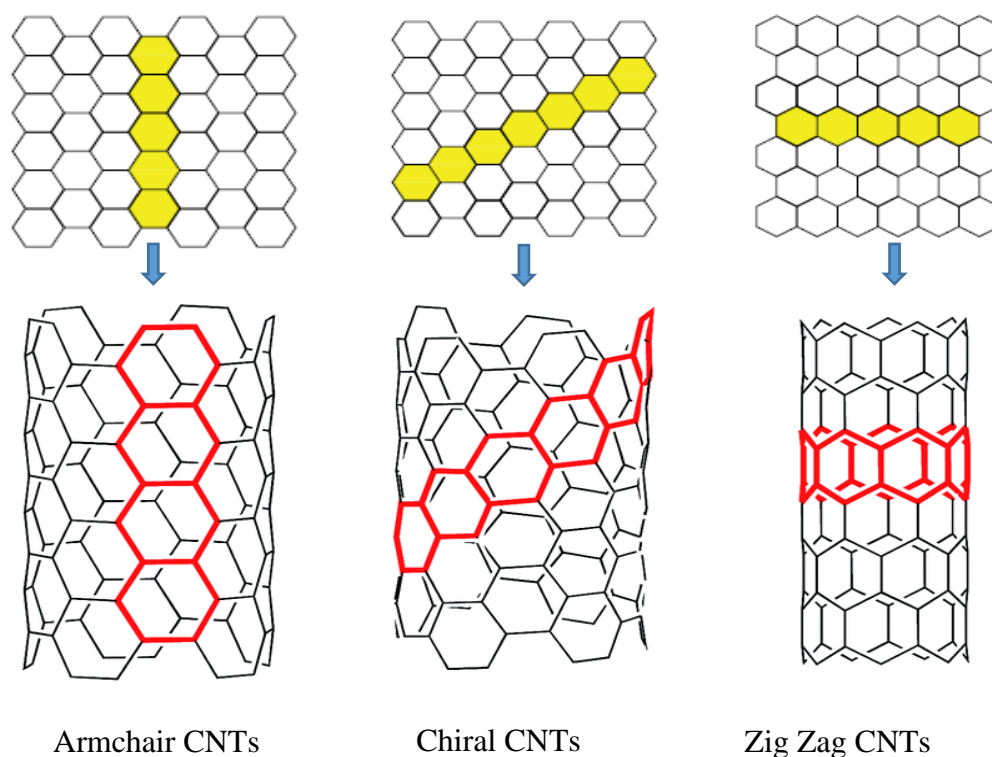


Figure 1.2 Classification of CNTs are armchair, chiral, and zigzag CNTs (J. Sisto et al., 2016)

1.1.1.2. Multi-Walled Carbon Nanotubes

Multi-walled CNTs (MWCNTs) are a stack of graphene sheets rolled up into concentric cylindrical structures (Khalid Saeed, 2013). MWCNTs can have as many as 50 layers of graphene (E.N.Ganesh, 2013). They have diameters ranging from 3 nm to 30 nm and can be centimeters long (Ákos Kukovecz, 2013). The inter-tube distance between layers is observed to be approximately 0.34 nm (Popov, 2004). A schematic diagram and a scanning electron microscopic image of MWCNTs is given in Figure 1.3 (b).

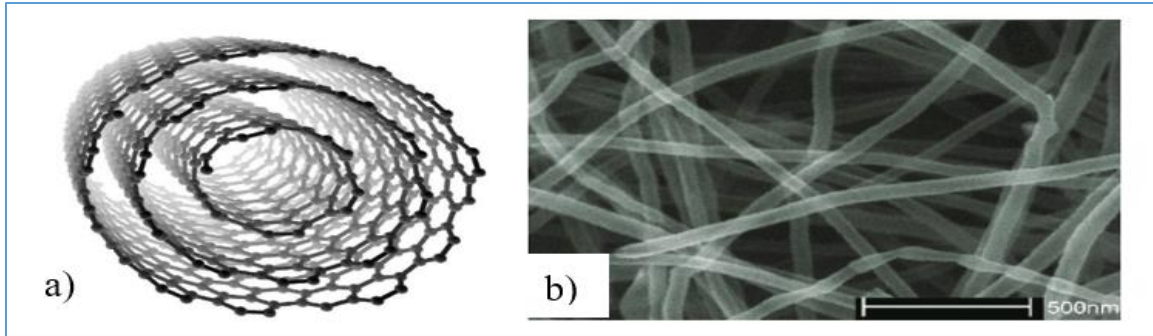


Figure 1.3 a) Schematic of multi-walled carbon nanotubes, b) Scanning electron microscopic image of raw multi-walled carbon nanotubes (Chen, 2016)

1.1.2. Properties of CNTs

1. Mechanical properties: CNTs are the strongest and stiffest material in terms of their strength and elastic modulus. CNTs are two orders of magnitude stronger than steel at 1/6th of their weight (Jorio et al., 2008). They are found to have a tensile strength of over 100 GPa and Young's modulus of 1 TPa (Yao & Lordi, 1998). Theoretically, they are found to be stiffer and more robust than any known substance. Experiments and simulations show a remarkable bend without breaking individual CNTs (Gogotsi, 2006). The high strength and stiffness arise due to interlocking carbon-carbon covalent bond or the σ bond.

2. Electrical properties: CNTs conduct electricity really well and are found to be better conductors than metals. The electron confinement along the nanotube circumference makes a defect-free nanotube either metallic or semiconducting (Meyyappan, 2004). The different carbon atom wrappings have a profound effect on the electronic properties. For example, armchair nanotubes as well as one-third of zigzag and chiral nanotubes, have electrical properties similar to metals while the remaining two-

third of zigzag and chiral nanotubes have the electrical properties of semiconductors (Cheap Tubes Inc., 2019).

3. Chemical properties: CNTs have a small diameter, large specific surfaces, and sigma-pi rehybridization, which shows strong sensitivity to chemical and biological environmental interaction. Hence the chemical properties of CNTs can be modified significantly, and they could be used for a wide variety of chemical and biological applications. Some of the chemical properties include opening, wetting, and filling, adsorption, charge transfer etc. (Meyyappan, 2004). Further, having a structure of carbon atoms closely aligned to graphene and their high degree of atomic-scale perfection makes them chemically inert.

4. Thermal and thermoelectric properties: Graphite and diamond show extraordinary heat capacity and thermal conductivity. For pure diamond, the thermal conductivity, k , is 2000 to 2500 $\text{Wm}^{-1}\text{K}^{-1}$, while for graphite, the in-plane conductivity at room temperature is about 2000 $\text{Wm}^{-1}\text{K}^{-1}$. Inherited from graphene, theoretical and experimental research studies show that CNTs also have exceptional thermal conductivity and stability at room and elevated temperatures. The thermal conductivity of CNTs is discovered to range between 2000 and 6000 $\text{Wm}^{-1}\text{K}^{-1}$ (Han & Fina, 2011). Further, at low temperatures, the thermal properties are found to be affected by phonons due to the effects of phonon quantization (Popov, 2004).

Overall experiments, theoretical studies, and calculations have shown that CNTs are small, extraordinary structures and possess a unique combination of excellent mechanical, physical, and chemical properties enabling them to be a right material choice for a wide range of promising applications. However, not all the CNTs possess

exceptional properties as they depend on the type of nanotubes, growth process, and fabrication methods.

1.2. Current Applications of Carbon Nanotubes

Applications of CNTs range from molecular electronics and quantum computing to materials science, energy storage, and medicine (Harris & Harris, 2009). The demonstrated high tensile strength and Young's modulus of nanotubes have led to their possible use in composite materials for structural applications with improved mechanical properties. CNTs are proving to be the best filler materials for nano-composites adding strength, electrical and thermal conductivity (Proctor et al., 2017).

The difference in chiralities and unique electronic properties for each form of CNTs allows for various device applications such as transparent electrodes for organic light emitting diodes (OLEDs), lithium ion batteries, supercapacitors and field effect transistors, rectifying diodes, and logic circuits (Schnorr & Swager, 2011). Further nanotubes are considered the central elements of electron devices, including electron field emitters, because of their high chemical stability, exceptional conductivity, and small size (Popov, 2004). CNTs are also being employed in biomedical applications for their fast response, low power consumption, long life, small size, and better performance. Some of the biomedical applications where CNTs play an important role are on radio oncology to generate X-rays, biological sensors to detect DNA sequences in the body, flow sensors to measure gases utilized by respiratory apparatus, bio probes to investigate remote region or cavity, drug delivery where CNTs can act as carrier for drugs to enter the nuclei, implantable nano sensors, nanotube-based actuator for artificial muscle devices etc. (Sinha & Yeow, 2005). Some of the applications of CNTs are represented in Figure 1.4.

Further, the use of CNTs for thin-film applications are emerging and offers a broad range of device-based applications. Thin films composed of CNTs are primarily used in large-area coverage electronics, transparent conductive heater films, flexible electronics such as sensors or integrated circuits (Hirotsu & Ohno, 2019).

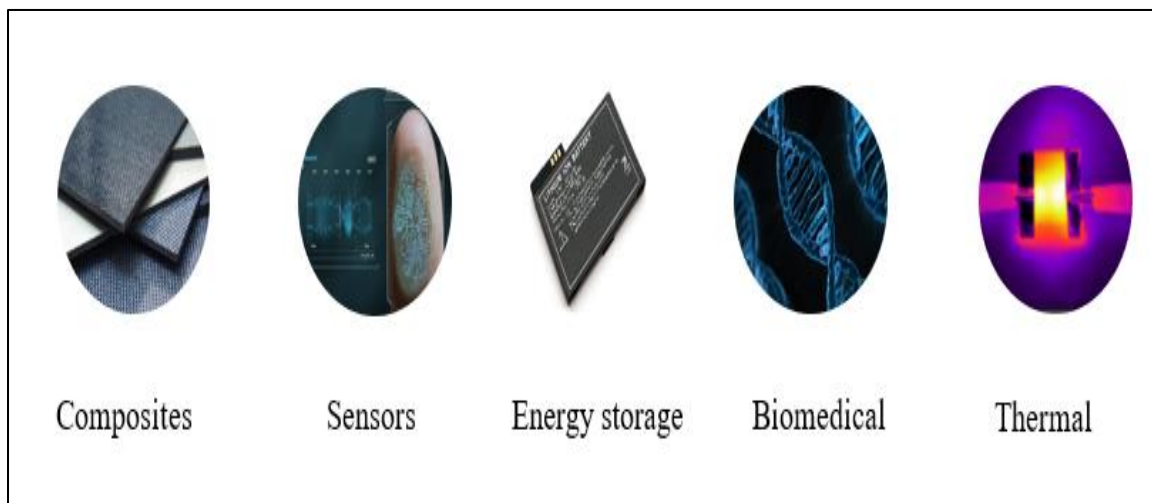


Figure 1.4 Application of CNTs in composites, sensors, energy storage devices, biomedical and thermal devices.

1.3. Aim of this Research

Thin films made of CNTs are currently an emerging field of research and offer a broad range of applications. This thesis mainly aims to develop and analyze carbon nanotube-based films for heating applications that can be used for de-icing and defrosting purposes. The advantages of CNT-based thin films include better reproducibility, high performance, readiness to integrate into devices (Wang & Moriyama, 2011). The collective behavior of random network of CNTs yields a film of superior physical properties and enhanced device performance.

1.4. Need for this Research

1.4.1. Limitations of Conventional Materials

In recent years, many advancements have been made in the thin film area to develop visibly transparent heaters for applications in optical-electronic devices, de-icing and defogging windshields using conventional materials. The most conventional material used for thin-film transparent heaters is Indium tin oxide (ITO). The advantages of ITO include high transparency (~90%) and conductance (~10 Ω /sq). However, ITOs are brittle in nature and cannot perform better at high temperature, restricting their inflexible and high-temperature applications (Gupta et al., 2016).

Eventually came the advent of graphene-based heaters and metal nanowire-based transparent heaters. Graphene-based heaters are low cost heaters that are light in weight. Since graphene has high thermal conductivity, these heaters show a good thermal response. However, they exhibit a high sheet resistance and require a large driving voltage to produce heat. Research and studies have been made to significantly lower the film sheet resistance and improve the transmittance of graphene-based heaters. However, graphene-based heaters produce excess joule heating, which results in non-uniform temperature distribution over large areas. On the other hand, metal nanowire heaters show a higher temperature with lower power input. However, these heaters show possible electrical failure at high surface temperatures, and joule heating ability is limited due to uneven current densities (Gupta et al., 2016).

To overcome these difficulties, current experimental and numerical research shows that CNTs are an excellent choice of materials compared to the conventional materials for the development of transparent film heaters. In this research, a unique process is

developed to fabricate thin carbon nanotube films and analyze their thermal and electrical properties.

1.4.2. Demand in Aircraft and Automotive Applications

The winter weather can wreak havoc on communities experiencing snow and ice. Ice especially can be very disruptive, downing power lines and rendering roads slippery. Ice can accumulate on propeller and rotor blades, on turbine blades, inside fuel lines, on pitot and angle of attack probes, as well as in carburetors, as shown in Figure 1.5. Icing has been recognized as a significant aviation hazard that can lead to increased aerodynamic drag and weight, along with a reduction in lift and thrust. Together all these factors may result in a higher stall speed and degradation of aircraft performance.



Figure 1.5 Icing on the windshield, leading-edge, and propeller blades (Briefing, 2020)

According to a news article (Duchon, 2014), there were over 750 airplane accidents due to icing between 1981 and 2009 (Figure 1.6). These issues are so important that the aircraft de-icing and anti-icing market is predicted to be worth \$1.3B by 2020 (MarketsandMarkets, 2015).

Commercial and business jets are usually equipped with de-icing and anti-icing devices for most of the systems mentioned above, but smaller general aviation airplanes may be equipped with only a few systems if any, at all. Pitot heat and carburetor heat are

commonly installed on small general aviation airplanes (e.g., Cessna 172 and Piper Cherokee), but leading-edge de-icing is limited to larger planes or as options on high-end planes (e.g., Cirrus SR22, Cessna Caravan, and Beechcraft Baron). Small planes are usually not certified to fly into known icing conditions, but that does not mean it never occurs. Moreover, when it occurs, ice accumulation can be swift and fatal.

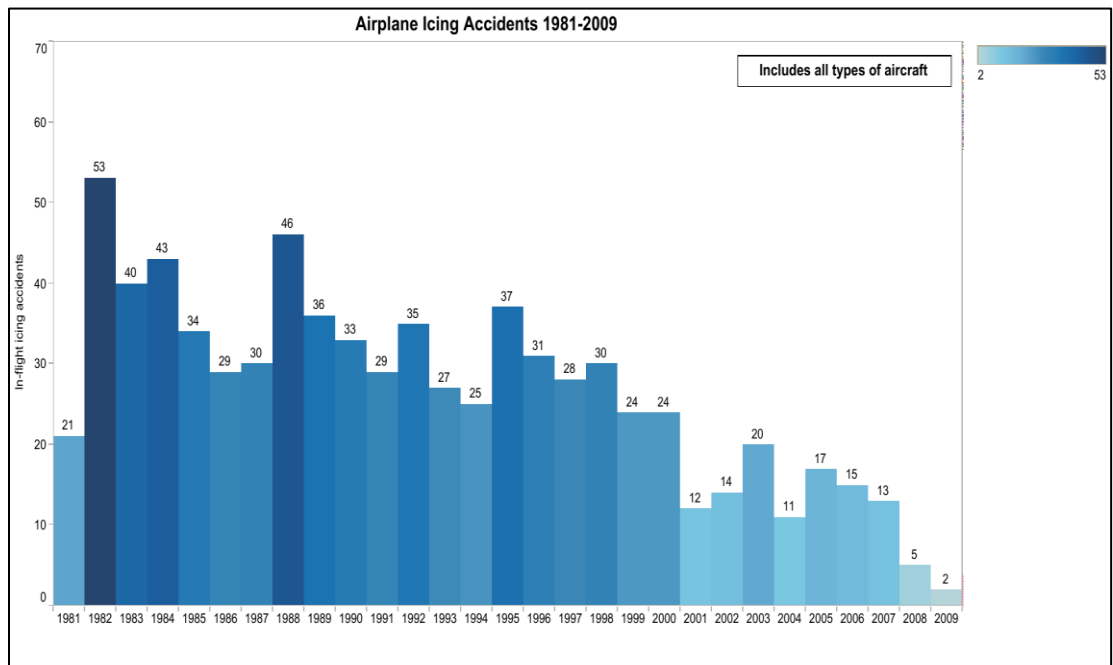


Figure 1.6 Aircraft icing accidents from 1981-2009 (Duchon, 2010)

Some of the drawbacks of current de-icing and anti-icing systems are their weight or their impact on engine efficiency. Jet aircraft commonly use bleed air from the engine to melt the ice, which reduces the engine power available for thrust. Inflatable boots need their own actuators and can only be used as de-icing devices. As the boots do not prevent ice from returning, they may need to be used several times throughout the flight. A more promising alternative is to use a heating element in the structure of the wing to melt the

ice. These methods are usually not easily adapted on smaller aircraft because they are either too expensive or their weight penalty is too significant for aircraft with an already small useful load. CNTs have been used as heaters in laboratory experiments. However, laboratory experiments may not scale well to large surface areas, need to be combined with other materials (Kim et al., 2017), or may not be suitable to apply in the field as a retrofit (Kang et al., 2011). The method we have explored would allow us to spin coat solution that would keep the film transparent and produce rapid heat upon applying a current through electrodes.

1.5. Motivation of Research

The present study is motivated by several open questions. CNTs are mainly known for their excellent thermal and electrical conductivities and might prove to be the best heating elements ever known to humankind. This remarkable property allows CNTs to be utilized as a potential electrothermal film heater for de-icing, defrosting applications, and various other functional devices. However, CNTs in their raw form possess many defects (Jeon et al., 2011) and tend to agglomerate due to strong Van der Waals forces. Hence raw CNTs themselves cannot be used for thermal heating applications but require modifications or need to be combined with other compounds. However, modification of CNTs with certain compounds has several limitations that include depleting the structure of CNTs and degrading the properties of CNTs, further being hazardous to health and the environment (Jang & Hwang, 2018).

Hence this study aims to find a unique modification process that not only preserves the electrical and thermal properties but also enhances the electrothermal properties while improving the solubility. Despite numerous studies focused on using CNTs for

electrothermal heaters, relatively few/none of them have investigated how the modification parameters affect the electrical resistance and the performance of the thermal heaters, to the best of our knowledge. The developed process outlined in this research uses modified CNTs for the development of electrothermal heaters, and this approach is proving to be a promising method for developing transparent electrothermal heaters with increased efficiency.

1.6. Importance of Research

The importance of this research is to develop a modification process that improves the solubility of the CNTs and further enhances the electrical characteristics of CNTs. In this study, we aim to modify the CNT non-covalently, investigate the influence of the polyaromatic moiety concentration, pH on current-induced heating and study the thermal behavior of the thin film. To date, there have been many experimental studies on the temperature profiles, or the current (I)-voltage(V) (IV) characteristics of CNT based thermal heaters (Jia et al., 2018). However, these experimental investigations have failed to provide a clear picture of the effect of amount of polyaromatic moiety and pH on the thermal conductivity of the CNT based heaters. In this research, we investigate the effects of the polyaromatic moiety and pH on current-induced heating experimentally and hypothesize on the reasons behind those effects.

1.6.1. Objective

The main objective of the study is to examine a novel technique on non-covalent functionalization to improve the performance of SWCNT film heaters. Here we aim to fabricate a thin SWCNT film on a glass substrate that could produce significant heat with a less amount of power.

1.6.2. Outline of Chapters

Chapter 2 gives a detailed explanation of the materials used and research procedure. Chapter 3 mainly focuses on the testing methods, experimental setup, and results. This chapter helps to understand the significance of the current research approach. The last chapter discusses the variations in the obtained measurements and possible reasons to understand the statistical errors. This thesis summarizes a new approach to functionalize CNTs, methods to fabricate thin-film heater, analyzes their electrothermal properties, and explains the future scope of this study.

2. Research Methodology

2.1. Research Approach

The purpose of this research is to fabricate and analyze the behavior of transparent film heaters based on CNTs and develop means of utilizing them for de-icing and defrosting applications. If successful, CNT film heaters may prove to have higher efficiency, longer operational life, and uniform heat distribution at lower power of 20 V compared to traditional heaters. It also provides the ability of the material to be used in different flexible substrates and complex geometries.

The research methodology is broken down into three main sections to fabricate the transparent film heater. To achieve this, first, a well-dispersed solution of CNTs are fabricated employing chemical methods. The prepared solution is utilized for thin film fabrication employing spin coating. Finally, the fabricated film is tested for voltage and current characteristics and investigated for their thermal response. The following section discusses the materials used, solution synthesis procedure, thin-film fabrication methods, and testing methods in detail.

2.1.1. Synthesis of SWCNT Solution

Raw CNTs are synthesized by various methods. The most common procedures for producing CNTs are the chemical vapor deposition method (CVD), laser ablation technique, and carbon arc discharge technique (Eatemadi et al., 2014). These synthesis methods often produce CNTs of different chiralities and diameters and are usually contaminated with metallic and amorphous impurities (Jeon et al., 2011). Also, during the synthesis, defects and abnormalities are generally observed. These impurities and defects in bulk disrupt the electronic and transport properties of CNTs (Algharagholy, 2019).

Further, CNTs strongly attract each other and tend to agglomerate due to weak interaction forces called the Van der Waals forces. In addition, CNTs are also found to have different surface energies that are difficult to characterize than organic solvents and polymers (Song & Youn, 2005). This reduces the chemical affinity of CNTs with other organic solvents or polymers. Surface energy is an important parameter that demonstrates the ability of the CNTs to have surface interactions and functionalization (Li et al., 2019).

Hence to overcome these practical obstacles, appropriate post-processing chemical methods are required to prevent them from bundling and get favorable electronic, mechanical, and thermal properties. These post-processing methods are known as modification techniques. The chemical modification of CNTs with other materials is called the functionalization of CNTs. The functionalization of CNTs with suitable compounds gives rise to nanotubes with much more enhanced properties and further expands its application.

2.1.1.1. Functionalization Methods

CNTs can be functionalized in various methods in order to precisely enhance the properties of the final materials. Currently, many research methods have been developed to functionalize CNTs. There are two predominant classifications of functionalization techniques that can be implemented for the improvement of the degree of reactivity and to attain homogeneous dispersion. These are called the covalent functionalization and non-covalent functionalization method. The functionalization technique introduces a specific compound or functional group on the structure of CNTs (Khalid Saeed, 2013). A general classification of functionalization methods is depicted in Figure 2.1.

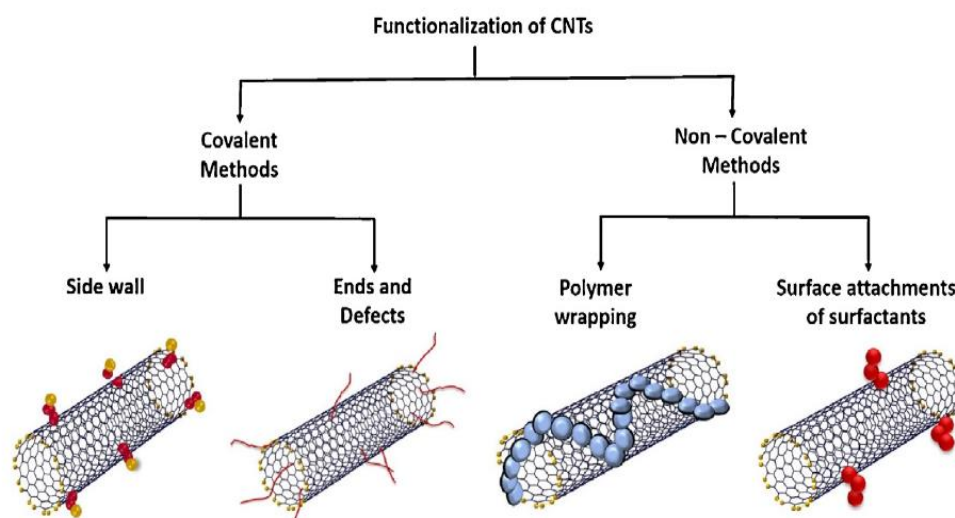


Figure 2.1 Representation of different methods of functionalization of CNTs (Karimi et al., 2015)

2.1.1.1.1. Covalent Functionalization

Covalent functionalization is based on the attachment of desired functional groups to the walls of CNTs. The functional group gets covalently bonded to the carbon nanotube structure at the end caps of CNTs or the sidewalls of CNTs. The functionalization can be achieved by using organic solvents or by oxidation methods. Various chemical groups that are used for functionalization are fluorine, carboxylic, p-aminobenzoic acid. The advantage of covalent functionalization includes good solubility of CNTs in various organic solvents, and it could be attached to various polymeric materials (Khalid Saeed, 2013).

However, the main disadvantages are, due to the direct bonding of functional groups with high reactivity, a large number of defects are extensively created on the sidewalls of the CNTs and break the CNTs into smaller structures. This leads to the degradation of mechanical properties and the disruption of π electrons in the microstructure. The π

electrons are the ones responsible for electrical and thermal transport. Hence the disruption of π electrons in the covalent bond causes the electrons to scatter and thereby hinders the electron transport of CNTs. Further, the use of organic solvents is also environmentally unfriendly and hazardous in nature and hence hampering their potential for practical applications.

2.1.1.1.2. Non-Covalent Functionalization

Non-covalent functionalization is based on the Van der Waals forces and does not involve any sharing of electrons with the CNTs. Henceforth carbon bonds are not disrupted, and the conjugated system of sidewalls of CNTs is not destroyed. It mainly involves electromagnetic interactions with the added nonfunctional group. While covalent functionalization results in degradation of properties, non-covalent functionalization on the other hand helps in enhancing and preserving the interfacial properties of CNTs. It also improves solubility quite remarkably. Hence this method is considered to be the most preferred type of functionalization (Jeon et al., 2011).

Non-covalent functionalization can be achieved using surfactants, polymers by employing $\pi - \pi$ stacking or hydrophobic interactions, and aromatic compounds with super-acids. The use of polymers has the advantage to be used as an excellent wrapping of material around CNTs, and surfactants have an advantage of reducing the surface tension and hence effectively results in uniform dispersion of CNTs. However, they are toxic in nature and potentially limited to consumer applications. On the other hand, aromatic molecules such as pyrene, porphyrin (Morishita et al., 2010), and their derivatives can interact with the sidewalls of CNTs by $\pi - \pi$ stacking interactions and hence leading up the way for non-covalent functionalization. In chemistry, $\pi - \pi$

stacking refers to attractive non-covalent interactions between aromatic rings that contains π bonds (“Pi-Stacking (Chemistry),” 2020). This method aids in improved solubility and efficient dispersion. Another method includes the use of super-acids along with the appropriate aromatic compounds. This results in having aqueous solutions of CNTs with improved and desired properties along with little or no structural damage. Hence aromatic compounds, along with super-acids are a promising nonfunctional group that could be used for modification where maximum enhanced properties could be expected and open up for many practical applications (Jeon et al., 2011). In this study, a novel non-covalent functionalization technique using super-acids and pyrene derived aromatic compound is implemented.

2.1.1.2. Chemical Materials Used

For this research, industry manufactured highly purified SWCNTs obtained from NanoIntegris Technologies, Inc. were used. The diameter of the obtained SWCNTs ranges between 0.8 to 1.2 nm, and length ranges from ~100 nm to 1000nm (“Small Diameter SWNTs (HiPco™),” 2020). 1-PyreneButyric Acid (PBA) 97% obtained from Sigma-Aldrich was used as the non-covalent functional group, and fuming sulfuric acid, 20% free SO₃ basis was used to create aqueous solutions of CNTs. Further, 20-30% ammonium hydroxide (NH₄OH) from Sigma-Aldrich and dilute ammonium hydroxide (NH₄OH) of pH 8.5 was used for neutralization and dilutions, respectively.

2.1.1.3. Solution Synthesis Methodology

For this research, two sets of experiments involving different ratios of CNTs to polyaromatic moiety were produced. In the first set of experiments, first 35 mg of SWCNTs and 35 mg of 1-pyrenebutyric acid were combined together in a small 20 mL

vial. Then, 10 mL of fuming sulfuric acid added was added dropwise into the 20 mL vial containing the mixture in ice bath. The solution was then stirred for approximately 10 hours at room temperature in ice bath. In this step, the polyaromatic moiety 1-pyrenebutyric acid gets combined with the SWCNTs in the presence of an acid. During this process, the fuming sulfuric acid works to break down the bundled CNTs, and the polyaromatic moiety gets non-covalently associated with the sidewalls of the SWCNTs. The acid helps create a solvating medium for the CNTs, and the pyrene attaches to the CNTs without breaking the π network of CNTs. Figure 2.2 represents the reaction between the pyrene group, CNTs, and superacid.

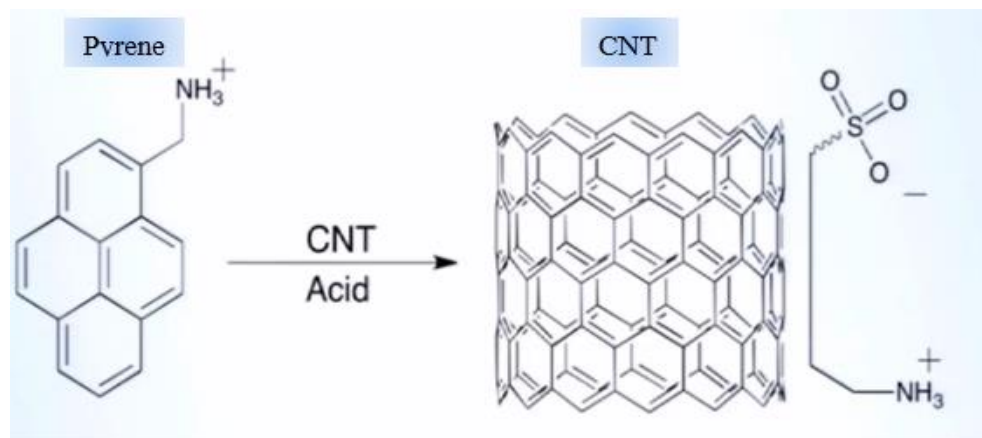


Figure 2.2 Non covalent functionalization of CNTs using polyaromatic moiety pyrene derivative and acid (Preparation and Properties of Carbon Nanotube-Based Inks, 2014)

The product of this reaction is the modified CNT, where the pyrene gets non-covalently attached to the sidewalls of the CNTs by means of Van der Waals forces, as shown in Figure 2.2. The resulting mixture of SWCNTs and 1-pyrenebutyric acid was then stirred to produce free-flowing and homogeneous suspension (Preparation and Properties of Carbon Nanotube-Based Inks, 2014).

This solution was then added dropwise into approximately 50 mL of deionized (DI) ice water. Further, weak base concentrated 28% to 30% ammonium hydroxide was added to obtain the desired pH. The solution was again stirred at room temperature for about an hour. After this process, the solution was diluted using approximately 5 mL of DI ice water and approximately 45 mL pH 8.5 ammonium hydroxide and then stored in the refrigerator at a lower temperature. The resulting solution was sonicated using an ultrasonicator for 7 hours to 8 hours depending on the dispersion of the CNTs at 3°C. The sonicated solution was then centrifuged at -3°C at 5000 rpm for 5 minutes. The supernatant of the centrifuged solution was disregarded, and the bottom residue of CNTs was taken with the addition of little amounts of pH 8.5 ammonium hydroxide. The resulting concentration of CNTs in the solution was found to be 0.1g/mL.

In the second set of experiments, the amount of PBA combined with CNTs is five times that of experiment 1. 35 mg of SWCNTs and 175 mg of 1-pyrenebutyric acid are taken in a small 20 mL vial and combined. Then, 10 mL of fuming sulfuric acid was added dropwise into the 20 mL vial containing the mixture in ice bath. The solution was then stirred for approximately 10 hours at room temperature in ice bath. This solution was added dropwise into approximately 50 mL of DI ice water.

Further, weak base concentrated 28 % to 30 % ammonium hydroxide was titrated, and the desired pH was maintained. The solution was stirred at room temperature for about an hour. After this process, the solution was further diluted using approximately 5 mL of DI ice water and approximately 45 mL pH 8.5 ammonium hydroxide and stored in the refrigerator at a lower temperature. The resulting solution was sonicated using an ultrasonicator for 7 hours to 8 hours, depending on the dispersion of the CNTs at 3°C.

The sonicated solution was then centrifuged at -3°C at 10000 rpm for 10 minutes. Solution samples of experiment 1 and experiment 2 before and after centrifuge are differentiated in Figure 2.3. The supernatant of the centrifuged solution is disregarded, and the bottom residue of CNTs was taken with the addition of little amounts of pH 8.5 ammonium hydroxide. The resulting concentration of CNTs in the solution was then found to be 0.1g/mL.

The final solution which we obtained was free-flowing, aqueous, and contains modified CNTs with PBA bonded to the sidewalls by Van der Waals force.

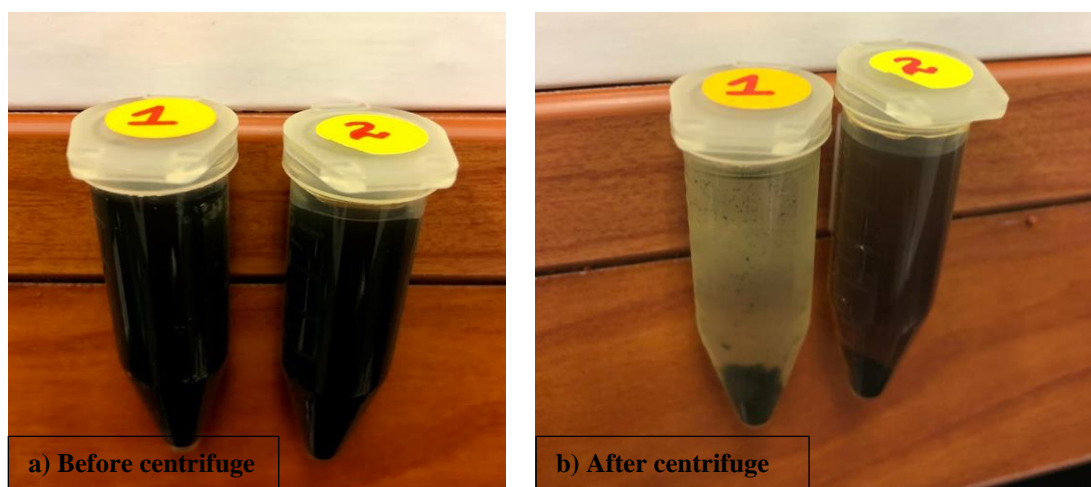


Figure 2.3 Solutions of experiment 1 and experiment 2 a) before centrifuge, b) after centrifuge.

2.1.1.4. Experiments Performed

For the first set of experiments, following the above-described methodology, three solutions were prepared while maintaining different pH during the addition of concentrated ammonium hydroxide. Similarly, for the second set of experiments, three solutions of different pH were prepared. The experiments performed here are the first of

their kind to study the influence of polyaromatic moiety PBA and the pH on the electrical properties of SWCNTs to the best of authors' knowledge. A total of six solutions were produced. The produced solutions, their names, composition, and pH maintained is given in Table 2.1 and Table 2.2. An image of the produced solutions of experiment 1 and experiment 2 is given in Figure 2.4

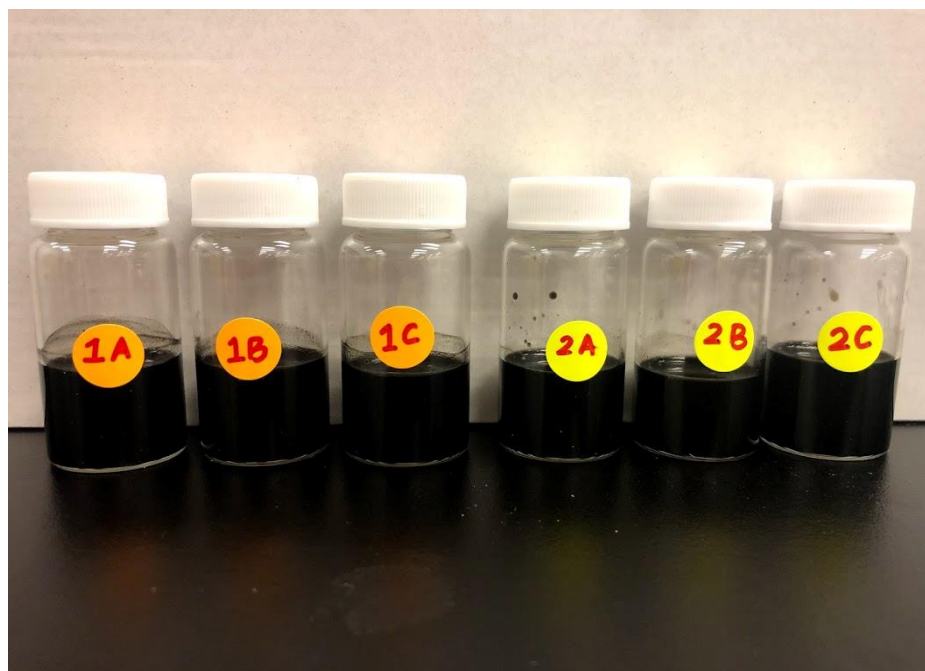


Figure 2.4 Fabricated solutions of experiment 1 and experiment 2

Table 2.1

Synthesized solution, pH, and amount of compounds in experiment 1.

Solution name	pH	Amount of CNT (mg)	Amount of PBA (mg)	The ratio of CNT to PBA
1-A	4.5	35	35	1:1
1-B	6	35	35	1:1
1-C	8	35	35	1:1

Table 2.2

Synthesized solutions, pH and amount of compounds in experiment 2

Solution name	pH	Amount of CNT (mg)	Amount of PBA (mg)	The ratio of CNT to PBA
2-A	4.5	35	175	1:5
2-B	6	35	175	1:5
2-C	8	35	175	1:5

2.1.2. Fabrication of SWCNT Films

The solutions prepared are now ready to be used for film fabrication. There are three main stages of the fabrication of SWCNT films:

1. Substrate preparation
2. Spin coating
3. Electrode application

2.1.2.1. Substrate Preparation

The first step in the film fabrication process is to choose an appropriate substrate and prepare the substrate so that it is clean, and hydrophilic. For this study, microscopic glass slides of size 2.5 cm length and 2.5 cm width were used as the substrate for coating the solutions. The glass substrates were first cleaned to remove any impurities and dust off the surface. The glass slides were first cleaned with soap and thoroughly rinsed with DI water. Further acetone was used to clean and dissolve any organic compounds. The glass slides were then ultrasonicated in ethyl alcohol for 10 minutes and then rinsed with DI water to remove any chemical impurities and to obtain high-quality films. Once the glass slides are cleaned, they were then treated for enhancing the hydrophilicity.

Different substrate treatments were performed to test the hydrophilicity of the glass substrate. Three batches of glass samples were taken and treated separately with acidic

piranha, basic piranha, and plasma treatment, respectively, and examined for the hydrophilic nature of the substrate. Among these treatments, the plasma treatment was the most effective and resulted in a lower contact angle and further enhanced wettability than piranha solutions. Hence the glass substrates for film fabrication are treated with oxygen plasma before coating with the CNT solutions. The oxygen plasma was applied to the glass slide for 1 minute and 30 seconds. The schematic representation of oxygen plasma applicator and plasma-treated glass slide is shown in Figure 2.5.

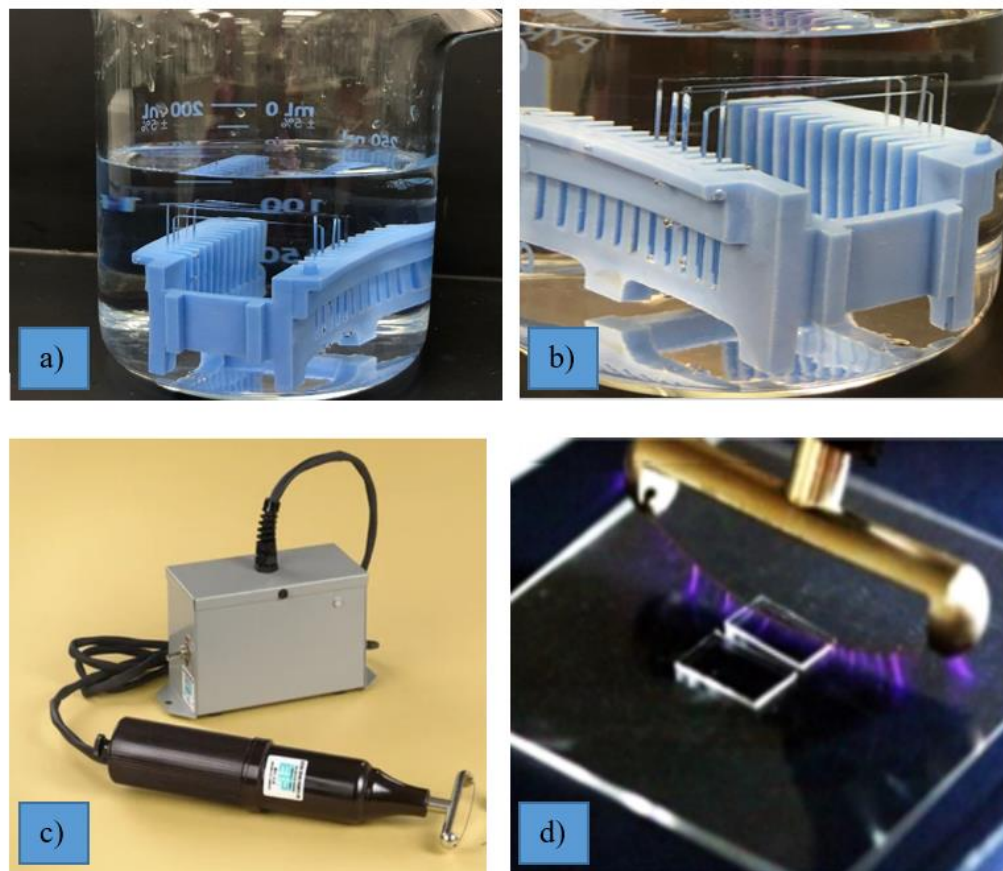


Figure 2.5 Preparation of the substrate before spin coating a) Cleaning of slides in DI water, b) Cleaning of slides with isopropyl alcohol and rinsing in DI water, c) Plasma applicator (BD-20AC Laboratory Corona Treater, 2020), d) Treating of cleaned slides with the application of plasma.

2.1.2.2. Spin Coating

There are different coating methods by which CNTs can be spread on the glass substrate. Different coating methods include dip coating, spray coating, and spin coating (Fu & Yu, 2014). In this thesis, the most common low cost, simple spin-coating procedure was implemented due to the ease of application and availability.

The spin coating technique is used for making thin uniform coating of organic materials on flat surfaces in the thickness range of nanometer to micrometer (Benelmekki & Erbe, 2019). There are four stages to spin coating, the first being deposition of the material on to the substrate, spin-up, spin-off and evaporation, as shown in Figure 2.6 (Al-Sharafi, 2019). In this process, first, the substrate is fixed to a plate or central chuck of the spin coater. The solution is then deposited onto the substrate by either static or dynamic dispensing. The substrate is then revolved at high speed. The resulting centrifugal force drives the liquid radially outward. The viscous force and surface tension result in solution of the material to be deposited on the substrate, and the film is formed by evaporation of the solvent throughout the process (Mishra et al., 2019).

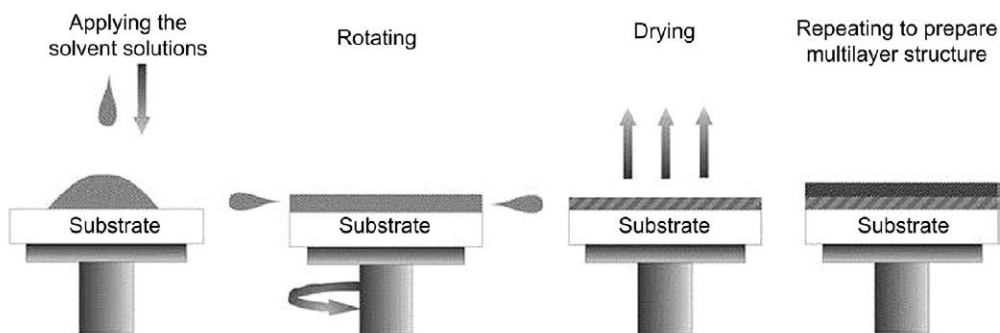


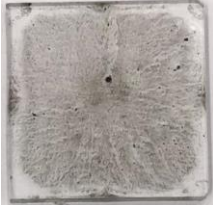
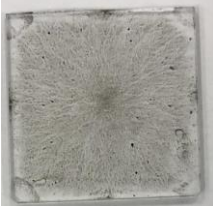
Figure 2.6 Schematics of steps involved in spin coating from application of solution to creation of thin films (Mishra et al., 2019).

The thickness of the film is controlled by angular speed, the viscosity of the solution, spinning time (Kumar & Nanda, 2019). In order to achieve a uniform thickness of the film, spin coating is performed at two stages, the first one at a low rotational velocity that is required to spread the solution over the substrate and eliminate possible air bubbles on the substrate, and the second stage is performed at high and specific rotational velocity (Castro et al., 2019). At this stage, high-speed spinning results in evaporation and thinning of the layer. This stage is followed by drying of the applied coating. The advantages of spin coating include low cost, flexibility to adjust the thickness of the coating, and also an excellent technique in a lab-scale environment. Further, there are a few disadvantages to this technique. The limitations include difficulty in creating multiple layers, in creating thin films of less than 10 nm, and impossibility of coating large substrates and loss of materials during spinning.

In this research, a two-stage spin coating technique is implemented. The plasma-treated glass substrate of 2.5 cm x 2.5 cm is placed on the central chuck of the Laurell 650 spin coater. Dynamic dispensing was used where the substrate first starts to spin at the required spin speed, and the solution is dispensed onto the center of the substrate. Dynamic dispensing is most often preferred because it is a more controlled process and consumes a minimal amount of solution. We tested different combination of spin speeds for the two-stage spin coating technique and used the combination that yielded uniform spread of solution on the sample. The different combination of speeds, the spin coated sample and the observations are tabulated in *Table 2.3*. The combination that worked best for the solution is Combination 4 (Combo 4). The first stage was set to spin at 2500 rpm for 10 seconds, and the second stage was set to spin at 2800 rpm for 30 seconds.

Table 2.3

Effect of spin speed combination on the resulting samples

Spin coated sample	Spin speed combination	Observations
	<u>Combo-1 Sample</u> Stage 1 : 500 rpm Stage 2 : 1500 rpm	<ul style="list-style-type: none"> - Edge effects - Streak pattern of CNTs on the substrate - More number of particles on the substrate
	<u>Combo-2 Sample</u> Stage 1 : 500 rpm Stage 2 : 3000 rpm	<ul style="list-style-type: none"> - Edge effect - Thin streak pattern of CNTs on the substrate - More number of particles on the substrate
	<u>Combo-3 Sample</u> Stage 1 : 1000 rpm Stage 2 : 3000 rpm	<ul style="list-style-type: none"> - Edge effect - Very thin streak pattern of CNTs on the substrate - Less number of particles on the substrate
	<u>Combo-4 Sample</u> Stage 1 : 2500 rpm Stage 2 : 2800 rpm	<ul style="list-style-type: none"> - Very minimum edge effect observed - No pattern observed on the substrate - Transparent, very fine particles on the substrate
	<u>Combo-5 Sample</u> Stage 1 : 2500 rpm Stage 2 : 3000 rpm	<ul style="list-style-type: none"> - Very minimum edge effect observed - No pattern observed on the substrate - Highly transparent, very few particles on the substrate - Not conductive

Approximately 0.5 mL of the solution was dynamically dispensed on to the glass substrate. Then the solution was spun off and evaporated in the second stage. Multiple layers were obtained by repeating the spin coating procedure where each layer was

allowed to dry for an hour before the next layer was coated. All the samples were coated with three layers using the same procedure.

2.1.2.3. Electrode Application

Once the glass substrate was spin-coated and dried with the prepared solutions, electrodes were applied on to the two edges of the glass slides. Electrodes were applied to the substrate to provide current and to measure the resistance of the film. In this study, a few samples used silver epoxy while the others used silver paint obtained from TedPella as their electrodes. The electrodes are applied on the opposite edges of the spin-coated film without disturbing the deposited CNT layers, as shown in Figure 2.7.

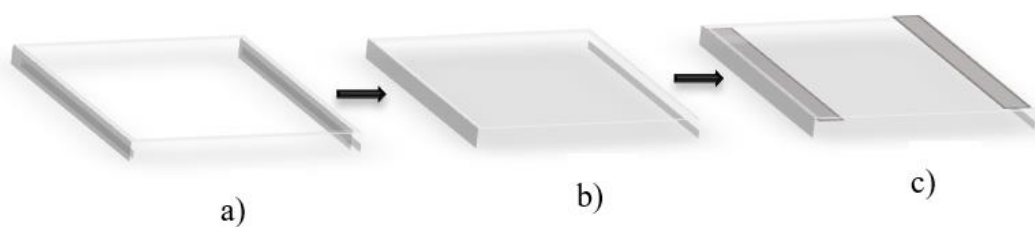


Figure 2.7 Schematic of fabrication of film heater a) Clean plasma treated glass slides, b) CNT spin coated glass substrate, c) Application of silver paint on the fabricated film.

2.2. Characteristics of Fabricated Film Heater

The fabricated film heater has a thin layer of carbon nanotubes on the surface of the glass substrate. The electrical properties of the sample depend on several characteristics, such as the size and geometry of solute particles, aspect ratio, and dispersion of nanoparticles in the solution and on to the substrate (Behnam et al., 2007). The uniform distribution of the nanoparticles on the substrate provides the potential for forming a

conductive pathway on the substrate. The lowest concentration at which the electrical pathway is formed throughout the sample is called the percolation threshold.

A fabricated film to function as a heater must possess low resistance such that it generates heat as current flows through it. Yeo-Hwan Hoon, in his study (Yoon et al., 2007), described how the length of CNTs affect the film resistance and transmittance. They observed that short CNTs lead to an increase in contacts between the networked CNTs, leading to an increase in overall film resistance. In this case, the transmittance of the film is traded off to obtain a film of low resistance. On the contrary, long CNTs quickly achieve the percolation network with high transmittance and low resistance. However, the geometry of the CNTs depends mainly on the CNT manufacturing methods, and most often, it is difficult to obtain long CNTs. In this study, we used industry made raw powder of SWCNTs of individual diameter ranging from ~ 0.8 nm to 1.2 nm and length ranging from ~ 100 nm to 1000 nm. Some of the spin-coated films are depicted in Figure 2.8.

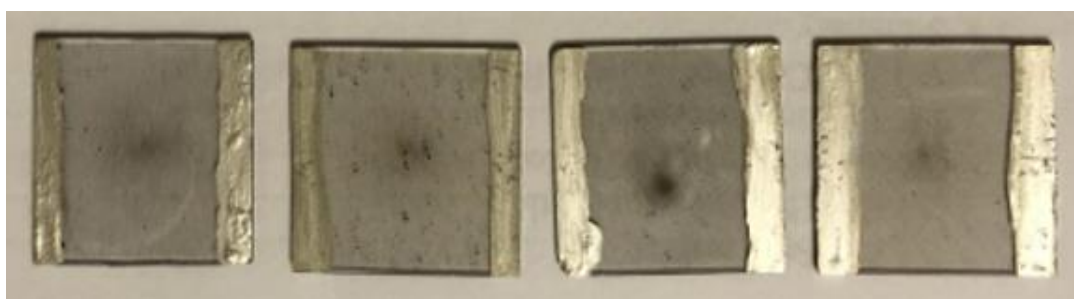


Figure 2.8 Spin coated samples of fabricated film heater

2.2.1. Heating Mechanisms

Carbon nanotubes are excellent electrical conductors (Costa et al., 2011). In this study, a solution containing SWCNTs were deposited on a glass substrate. Hence the resulting substrate contains a random network of SWCNTs on its surface. Several experimental studies and numerical models have been made to study the thermal energy transport properties in CNTs. A study by Chien, Cho, and Kumar revealed that with the application of various electric current ratings at a fixed length, carbon nanotubes exhibit joule heating (Chien et al., 2014). In contrast, a few other studies, as given in the review article shows that the thermal conductance is primarily dominated by phonons (Marconnet et al., 2013). Phonon heat transport exists at lower temperatures and at phonon mean free path in carbon nanotubes where the estimates of phonon mean free path ranges between 50 nm (Choi et al., 2006) to 1.5 μm (Hone, 2002). Hence as the temperature goes up, and the dimensions increase, the materials shift from a phonon conductor to a diffusive conductor (Marconnet et al., 2013). In diffusive conduction, the electrons are the charge carriers and conduct current. In this study, the fabricated film heater is of a macro-sized scale, and thermal properties are tested at room temperature. Hence the phonon conducting phenomenon does not apply to this study, and the heating phenomenon for the fabricated CNT film is primarily Joule heating.

2.2.1.1. Concept of Joule Heating

Joule heating, also known as ohmic heating, is a physical phenomenon by which thermal energy is produced utilizing electric current through an electrical conductor (What Is Joule Heating?, 2020). The primary means of conduction in this phenomenon is through movement of charge carriers or electrons. A difference in electromotive force

between two ends of a conductor drives the electrons in the material to move. The movement of the electrons depends on the number of free electrons and the resistance of the conductor material. Joule's law states that the heat developed in a conductor per unit time is proportional to the resistance of the wire and the square of the current.

$$\frac{H}{t} = I^2 R$$

$$P = I^2 R$$

Based on Ohms Law, $V = I \times R$

Hence the power becomes $P = \frac{V^2}{R}$

Where 'H' is the heat generated in time 't,' and 'I' is the current flowing through the conductor, and 'R' is the resistance of the conductor material. The heat generated per unit time is also known as the power of the electric conductor, 'P'. The heat generated is observed through temperature change along the conductor.

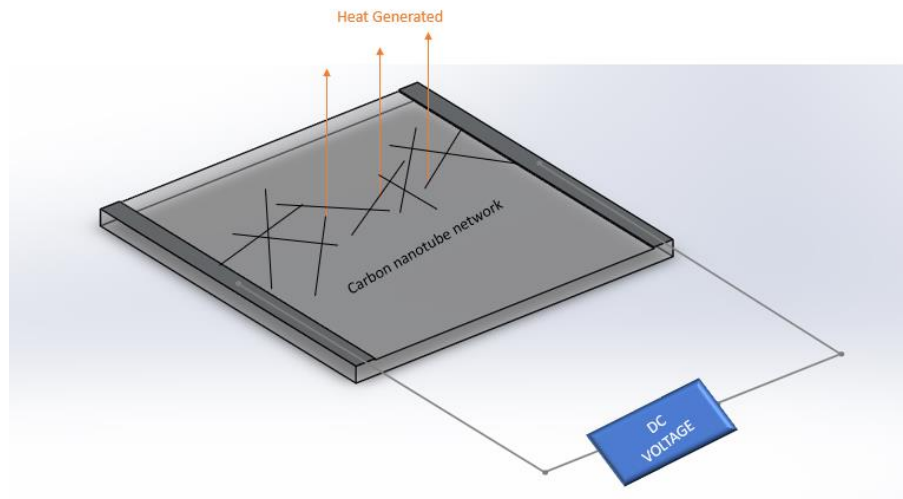


Figure 2.9 Model of carbon nanotube film heater and representation of heat generated due to the presence of network of CNTs

Here the CNTs deposited on the glass films act as electrical conductors and conduct heat as they carry current with the application of voltage (Figure 2.9). Based on the resistance of the film and the amount of current it can carry heat is generated in the film. For a given voltage, the film, which has the lowest resistance, produces the most amount of heat.

2.3. Summary

This chapter summarizes different functionalization techniques, the need for non-covalent functionalization, detailed procedure describing the non-covalent functionalization method used in this study. It further explains how the current modification technique enhances solvability and could be used for possible thin-film heater applications. Finally, it discusses the fabrication of a carbon nanotube-based thin film heater and describes the heating phenomenon in the developed film heater.

3. Testing and Results

3.1. Testing Methods

Several samples were produced and prepared for testing using the procedure described in the Section 2.1. The final quantities of prepared samples to be tested are given in is given in *Table 3.1*. The samples were tested for their resistance and temperature profile, power, and transmittance values.

Table 3.1

Quantity of samples prepared for experimental sets 1 and 2 using silver paint and silver epoxy as electrode

Samples prepared using silver paint as electrode	Quantity of samples	Samples prepared using silver epoxy as electrode	Quantity of samples
1-A	3	1-A	3
1-B	3	1-B	0
1-C	3	1-C	3
2-A	3	2-A	0
2-B	3	2-B	3
2-C	3	2-C	3

3.1.1. Resistance Testing

The above-listed samples were used to test the current flow characteristics of thin films of carbon nanotubes. These samples are tested to ensure that the fabrication process was successful. The uniform distribution of the nanoparticles on the substrate would provide the potential for the formation of conductive pathway and the samples were tested to see if there is any electrical connection and conducting path between the electrodes on the sample. Any specimen which shows negative or inconsistent value will not be used for further testing and analysis.

To accomplish this, each sample was connected to the Keithley 2612 B source meter. The Keithley source meter was used to supply the required DC voltage, and Kickstart software was used to analyze the current, power, and resistance values. The resistance was observed for all the samples with a power supply of 0.1 V. 1000 resistance measurements were taken for each sample using the source meter, and the average of those measurements were taken as the film resistance. The standard deviation is obtained for these 1000 resistance measurement counts made on each sample. The sample resistance values were further plotted and compared.

3.1.1.1. Resistance Test Results

The fabricated films were tested for their electrical conductivity. In this testing procedure, some samples of the same experiment exhibited high values of resistance in the range of $10^6 \Omega$ to $10^9 \Omega$ with a high standard deviation. A bar graph shown in Figure 3.1 and Figure 3.2 is plotted to compare different samples of experiments 1 and 2. In this graph, each bar of the same color represents an experiment of specific pH. For example, in Figure 3.1, three orange bars on the left side represent samples of experiment 1-A of pH 4.5, an acidic pH; the center three dark yellow bars represent samples of experiment 1-B of pH, close to neutral pH. The right most three bars of green color represents samples of Experiment 1-C of pH 8, a basic pH. We have fabricated three samples for each experiment in experiments 1 and 2 with silver paint as the electrode. Hence in the bar graphs represented, each bar of the same color named 1, 2, and 3 are different samples of the same experiment. For example, in Figure 3.1, amongst the first three orange bars, the first bar named 1 represents sample 1 of experiment 1-A. The second orange bar named 2 represents sample 2 of experiment 1-A, and the third orange bar

represents sample 3 of the same experiment 1-A. Since different experimental samples showed different values of resistance, the y-axis is kept as a log scale in Figure 3.1, Figure 3.2, and Figure 3.3.

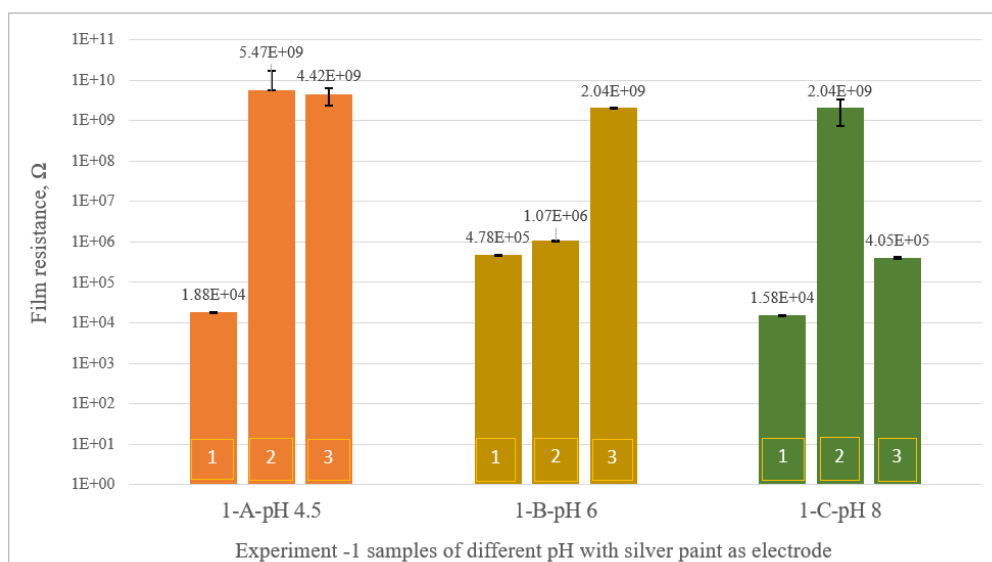


Figure 3.1 Resistance of CNT film samples of experiment 1 with silver paint as electrode

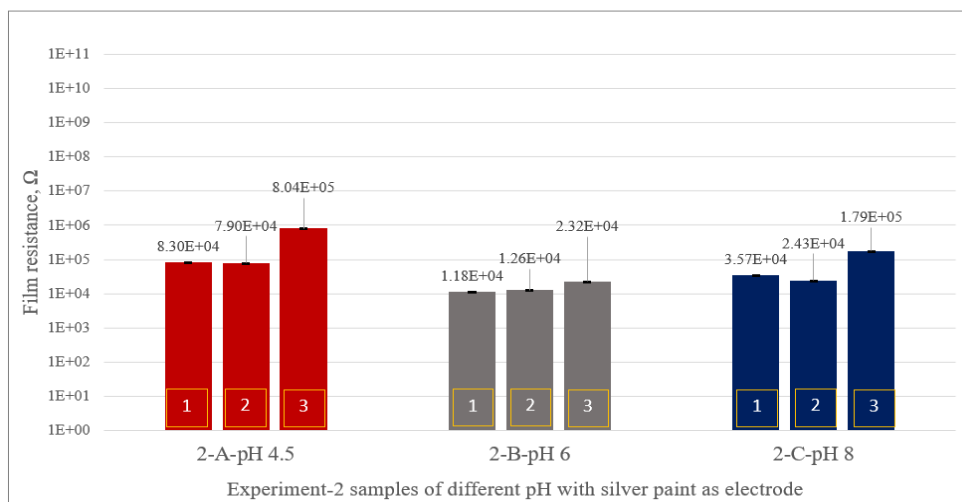


Figure 3.2 Resistance of CNT film samples of experiment 2 with silver paint as the electrode.

First, the samples of experiments 1 and 2, which had silver paint as electrodes, were tested to see if the conductive network is established. From Figure 3.1 and Figure 3.2, we can see that samples which demonstrated high resistance were sample 2 and 3 of experiment 1-A, samples 1,2, and 3 of experiment 1-B, sample 2 of experiment 1-C. Similarly, samples 1,2, and 3 of experiment 2-A, sample 3 of experiment 2-C exhibited high resistance greater than $10^5 \Omega$. The resistance values of other film samples were relatively lower in the order of $10^4 \Omega$.

The relatively high resistance and high standard deviation values in the samples were caused by several factors. Factors that might cause the high standard deviation were the nonuniformity of distribution of SWCNTs on the glass substrate during spin coating, wearing of silver paint electrode on the glass substrate during multiple testing procedures, and dispersion of SWCNTs not being uniform in the fabricated solution. The non-uniform spread of SWCNTs in the film occurred due to spin coating. During spin coating, some areas on the film resulted in having a higher concentration of the SWCNTs, mainly about the center of the substrate and edges having a relatively lower distribution of CNTs. This eventually affects the conductive path that is established by the network of CNTs, leaving some sites with less/without CNTs. The uniformity of dispersion depends on the density of the solution and its ability to adhere well to the glass substrate. These vacancies cause the film heaters to have high resistance value, and also a relatively higher deviation in resistance values could be possible.

Moreover, the relatively high resistance of the fabricated films is also due to non-uniform distribution on the sample. If the sample has vacant spots, it means there are not enough CNTs to provide a conductive network, and the resistance is increased. Similarly,

if the concentration of CNTs is more at a certain spot, there are increased network contacts between the CNT, which drastically increases the resistance. Further, the high resistance would have resulted because of the solution itself. During the experimental study, all the film samples could not be produced on the same day, and in the process of research and experimenting, all the samples were not prepared at the same time. Hence during the spin coating procedure and fabrication of film, solutions were ultrasonicated for about an hour before the start of spin coating to ensure there are no large CNTs or clumping of CNT particles in the solution.

The ultrasonication process was proven to affect the electronic nature and properties of CNTs. Advani & Hsiao described that the intense ultrasonication process could possibly destroy the graphene layers in CNTs, lead to the formation of amorphous carbon fibers, and deplete the properties of CNTs (Advani & Hsiao, 2012). Hence, the samples prepared at a later period showed high resistance values. Certain factors could not be controlled during the experimentation process and resulted in large deviation and uncertainty in results. However, significant improvements are being made to establish a uniform nanotube network and reduce possible errors.

a) Influence of Polyaromatic Moiety: For the current study, only sample-1 of experiments 1-A, 1-B, 1-C, and experiments 2-A, 2-B, 2-C were considered since it was fabricated at an earlier period. Comparing sample-1 of experiment 1-A and 2-A of an acidic pH 4.5, the sample exhibited a lower resistance value of $1.88 \times 10^4 \Omega$, and sample 2-A exhibited a film resistance of $8.30 \times 10^4 \Omega$. Similarly, comparing sample-1 of experiment 1-C and 2-C, sample 2-C exhibited a higher value of resistance of $3.57 \times 10^4 \Omega$, whereas film 1-C exhibited film resistance of $1.58 \times 10^4 \Omega$. Samples of experiment 1-

B exhibited continually increasing values of high resistance with high standard deviation and hence were not considered for comparison with 2-B. Here in experiment 1-A, samples 2 and 3 had relatively a higher standard deviation than experiment 1-B. However, for experiment 1-A, the high standard deviation resulted because of negative values in measurements whereas for experiment 1-B standard deviation resulted because of continually increasing values of resistance.

From the above comparison, it could be seen that experiment 1, which had 1:1 weight percent of CNTs and PBA, demonstrated a lower resistance, and experiment 2, which had 1:5 weight percent of CNT: PBA, showed a higher resistance. Based on the results, it could be said that an increase in the amount of PBA increases the resistance of the fabricated film. Hence it could be predicted that the amount of PBA added to the SWCNTs during the synthesis of solutions play a major role in influencing the electrical and conductive properties of CNTs. Hence, with precise control of the amount of functional group added, film heaters of desired properties could be obtained.

Table 3.2

Resistance characteristics of CNT film samples of experiment 1 with silver paint as the electrode.

Samples	Resistance, Ω 1-A-pH 4.5	Resistance, Ω 1-B-pH 6	Resistance, Ω 1-C-pH 8
Sample-1	1.88E+04	4.78E+05	1.58E+04
Sample-2	5.47E+09	1.07E+06	2.04E+09
Sample-3	4.42E+09	2.04E+09	4.05E+05

Table 3.3

Resistance characteristics of CNT film samples of experiment 2 with silver paint as the electrode.

Samples	Resistance, Ω 2-A-pH 4.5	Resistance, Ω 2-B-pH 6	Resistance, Ω 2-C-pH 8
Sample-1	8.30E+04	1.18E+04	3.57E+04
Sample-2	7.90E+04	1.26E+04	2.43E+04
Sample-3	8.04E+05	2.32E+04	1.79E+05

Now considering samples of experiments 1 and 2, which have silver epoxy as the electrode, the resistance values of experiment 1 and experiment 2 are compared. The resistance characteristics of samples of experiment 1 and experiment 2 with silver epoxy as electrodes are graphed in Figure 3.3. Again, here a few samples had high resistance and high standard deviation. Sample 3 of 1-C had considerably larger resistance compared to others. All the samples of experiment 1-A displayed resistance in the order of $10^3 \Omega$ and were precise. In experiment 2, all the samples exhibited average resistance of $10^4 \Omega$ and all the samples displayed high precision in resistance for 1000 measurement counts.

Comparing experiment 1 and experiment 2, we observed that experiment 2 again had a higher resistance than experiment 1. For example, sample 1 of experiment 1-A had average resistance of $7.37 \times 10^3 \Omega$, and sample 1 of experiment 2-A displayed a resistance of $5.95 \times 10^4 \Omega$, and the same trend follows for sample 2 and 3 of experiments 1 and 2.

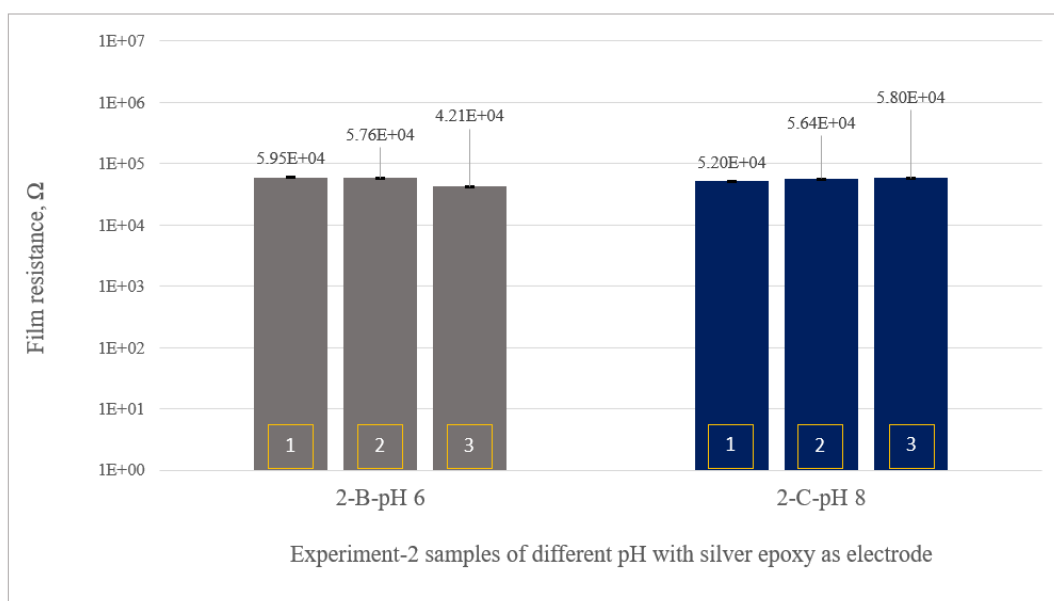
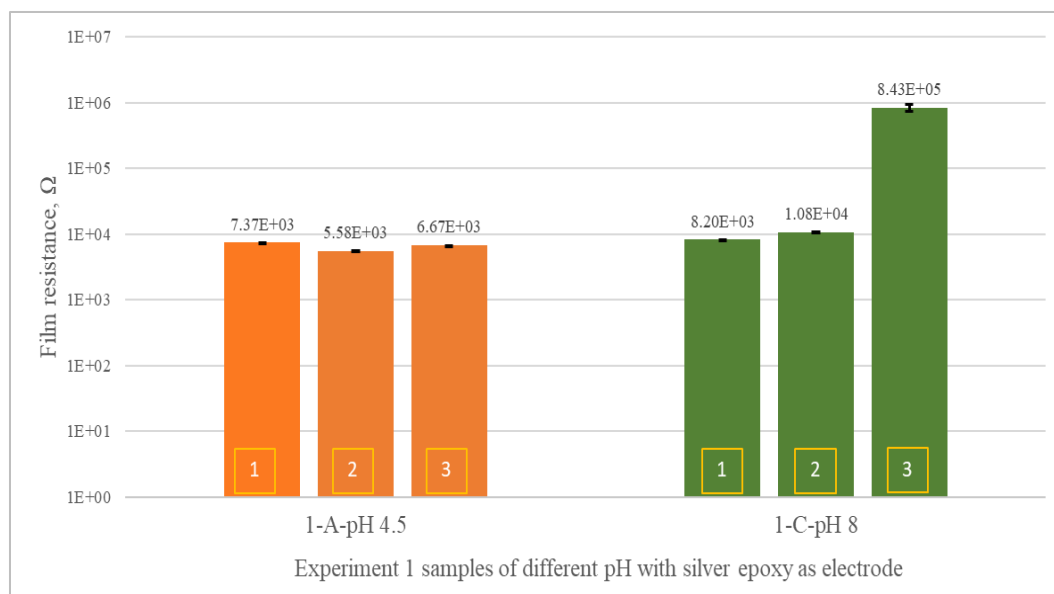


Figure 3.3 Resistance test results of experiments 1 and 2 with silver epoxy as electrode

b) Influence of pH: For each experiment, three solutions of different pH were prepared, and their resistance value was analyzed based on their pH. Analyzing Figure 3.1, Figure 3.2, Figure 3.3, no trend could be observed from our experiments. The

challenge here is that the pH value presented in this study is the pH maintained in step 2 of the experiment, and there are a series of dilutions performed, which alters the pH maintained at that step. Hence the final pH of the solutions was quite off from the measured pH. The impact of pH on the solutions could not be analyzed and was not carried forward in this research.

3.1.2. Electrothermal Performance Testing

The initial testing of resistance of thin films of CNTs was necessary as their responses to the power supply are responsible for generating heat. All the samples which had consistent resistance values were then observed for temperature profile. Each sample was connected to a 20 V power supply and was tested to see if the heat was generated across its entire surface. The heat generated was tested using FLIR E53 thermal camera. The FLIR camera captures the temperature of the samples at any location in the sample.

In this study, the samples were first placed in front of the FLIR camera at less than 1m. The temperature profile was observed and recorded using the ResearchIR software. The initial temperature of the samples was observed, and the power supply of 20 V was applied after a minute. The power supply was turned off after 15 minutes, and the cooling behavior was also recorded. The temperature profile was recorded for a total of 20 minutes, with the first one minute being the initial temperature response, the next 14 minutes giving the temperature rise with applied voltage and the last 5 minutes to observe the decrease in temperature across the CNT film heater.

3.1.2.1. Electrothermal Test Setup

The electrothermal test setup to observe the temperature rise in the film and to record the data is given in Figure 3.4. A block diagram of the electrothermal test setup is also

provided in Figure 3.4 for a better understanding of the setup. A Keithley source meter device is first connected to the Kickstart software via LAN cable, and then the required voltage is given as input to the Kickstart software. The software then provides the input to the source meter. The source meter leads are connected to the fabricated CNT film heater. Once the voltage is applied to the film heater through the source meter, the temperature increase was observed using the IR camera placed in front of the sample. The IR camera was connected to a laptop to record the measurements. ResearchIR software was used for recording the test. While this happens, the Kickstart software simultaneously collects the resistance, power, and current flowing through the film at the applied voltage.

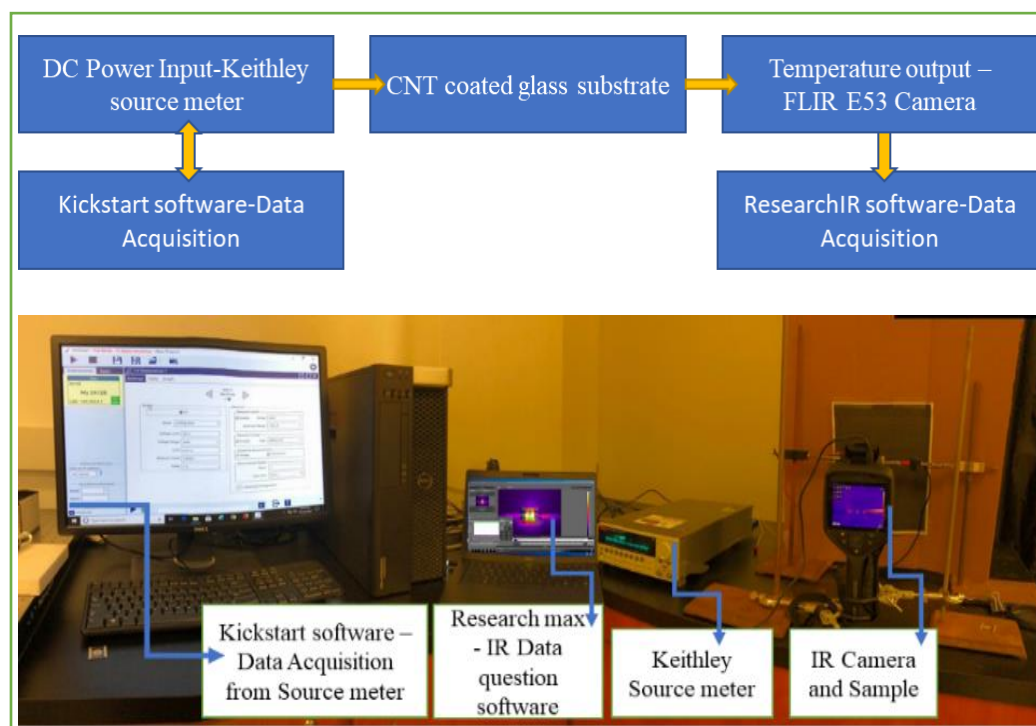


Figure 3.4 Block diagram representing the process involved in electrothermal testing (top), electrothermal test setup in the laboratory (bottom).

3.1.2.2. Electrothermal Test Results

A direct electrical power of 20 V was applied to the CNT film heater, and their electrothermal response was observed under ambient conditions. After electric power was applied to the films, the surface temperature rise happened without any delay and monotonically increased over time until a steady-state temperature was reached. As soon as the supplied electrical power was turned off rapid cooling as observed for all the samples which showed a thermal response. The electrothermal responses recorded under ambient conditions is graphed and compared.

For this analysis, only spin-coated sample 1 of experiments 1 and 2 with silver paint as electrodes is used for temperature measurements. Samples with silver epoxy did not adhere well to the surface of the glass substrate and tore off while clipping alligator clips to the electrodes. This, in turn, removes the CNTs deposited on the glass substrate and hence cannot yield exact results. For this reason, only samples of experiments 1 and 2, which used silver paint as the electrode were considered.

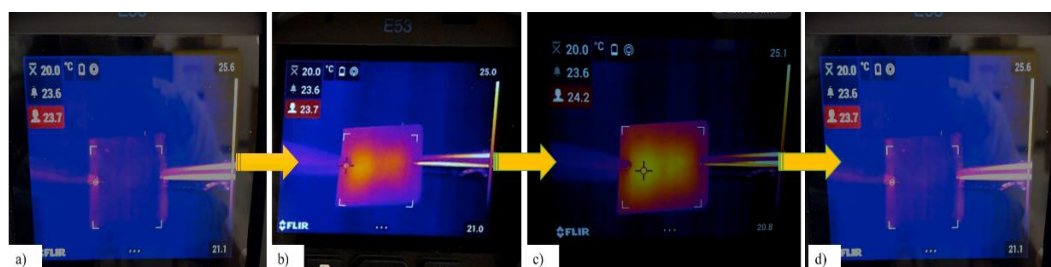


Figure 3.5 IR camera images of heat generation in fabricated film heater a) Film heater before application of voltage, b) Gradual heat generation after application of voltage, c) Uniform distribution of heat over the entire film, d) Film heater after the voltage was turned off.

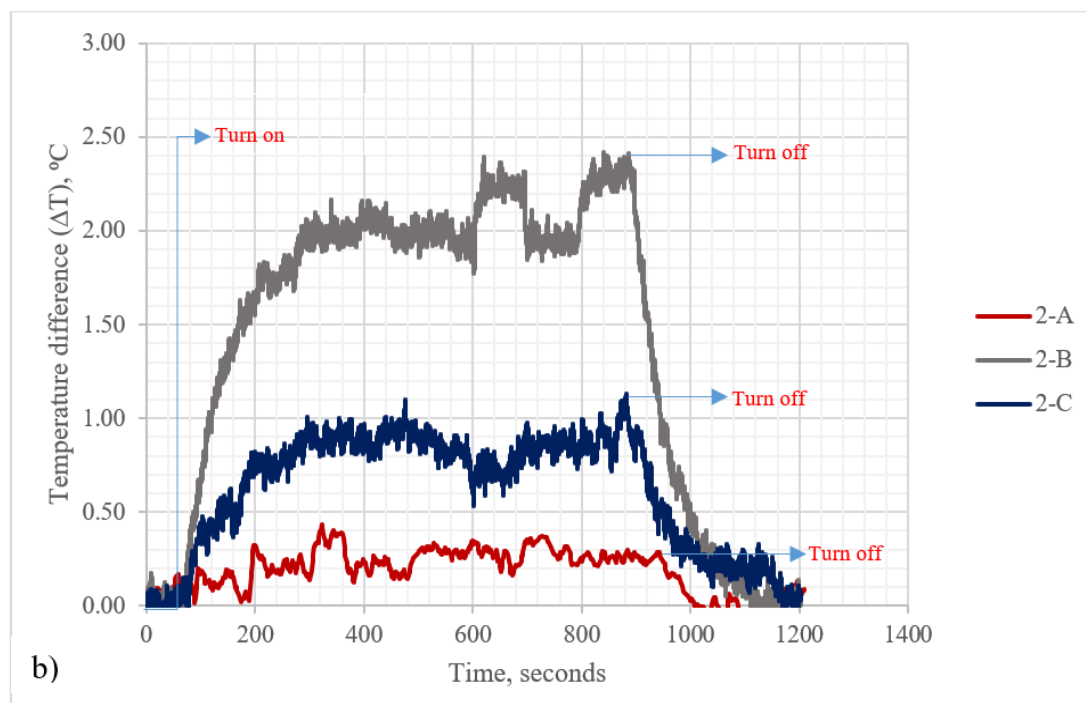
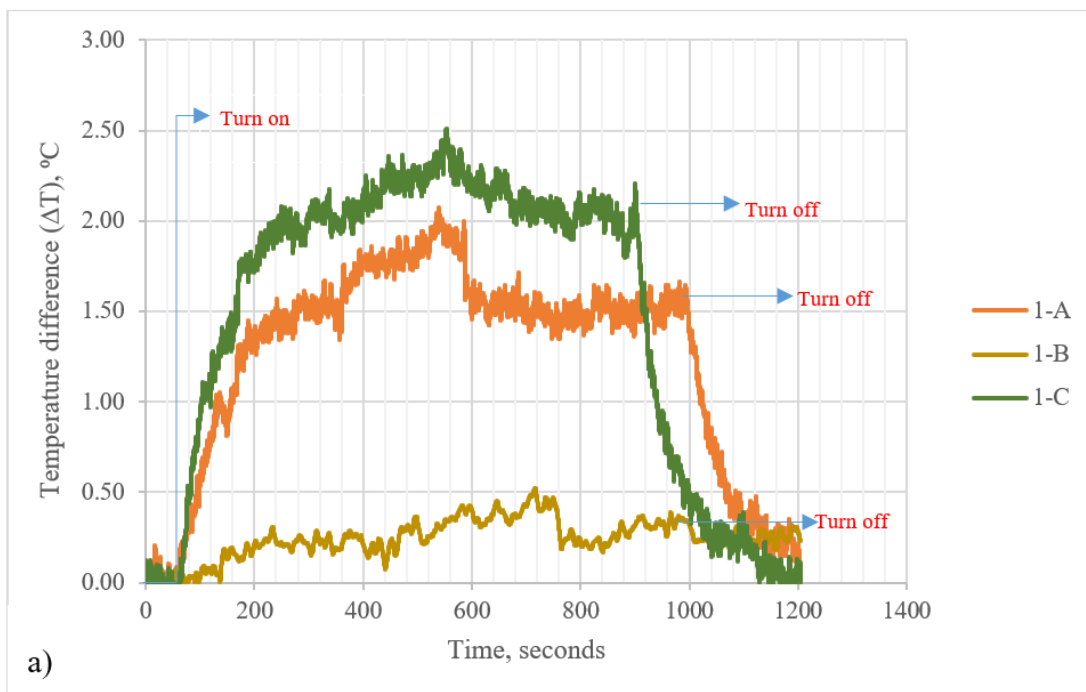


Figure 3.6 Temperature increase profile for CNT films of a) experiment 1 and b) experiment 2 at applied voltage of 20V

From Figure 3.6, it can be observed from comparing experiment 1-A and 2-A that 2-A relatively had very high resistance and the supply of 20 V of electric power was not sufficient to drive electric current across the heater to generate heat while experiment 1-A displayed a higher steady-state temperature and higher cooling rate. Similarly, comparing experiment samples 1-B and 2-B, 1-B had relatively high resistance greater than $10^5 \Omega$ and did not generate heat, and remained at room temperature. For experiments 1-C and 2-C, sample 1 displayed highest steady-state temperature and heating rate due to lower film resistance $1.88 \times 10^4 \Omega$.

The maximum temperature attained by the samples is shown in Figure 3.7 (a), and their response time is tabulated in *Table 3.4*.

Table 3.4

Tabulation of maximum temperature increase attained by each sample and their response time

Samples	Maximum temperature increase, °C	Response time, seconds
1-A	2.07	174
1-B	0.47	172
1-C	2.50	175
2-A	0.43	170
2-B	2.41	173
2-C	1.13	174

Here, the response time is calculated as time required to reach 90% of their steady-state temperature. The maximum temperature attained by sample-1 of experiment 1 and 2 greatly depends on the resistance. Figure 3.7 (b) shows the variation of maximum temperature increase due to film resistance. Film heater shows very minimal/no temperature rise at high resistance of $10^5 \Omega$ and displays maximum temperature rise at a

lower resistance value. Hence the maximum temperature rise was found to increase with decrease in the film resistance.

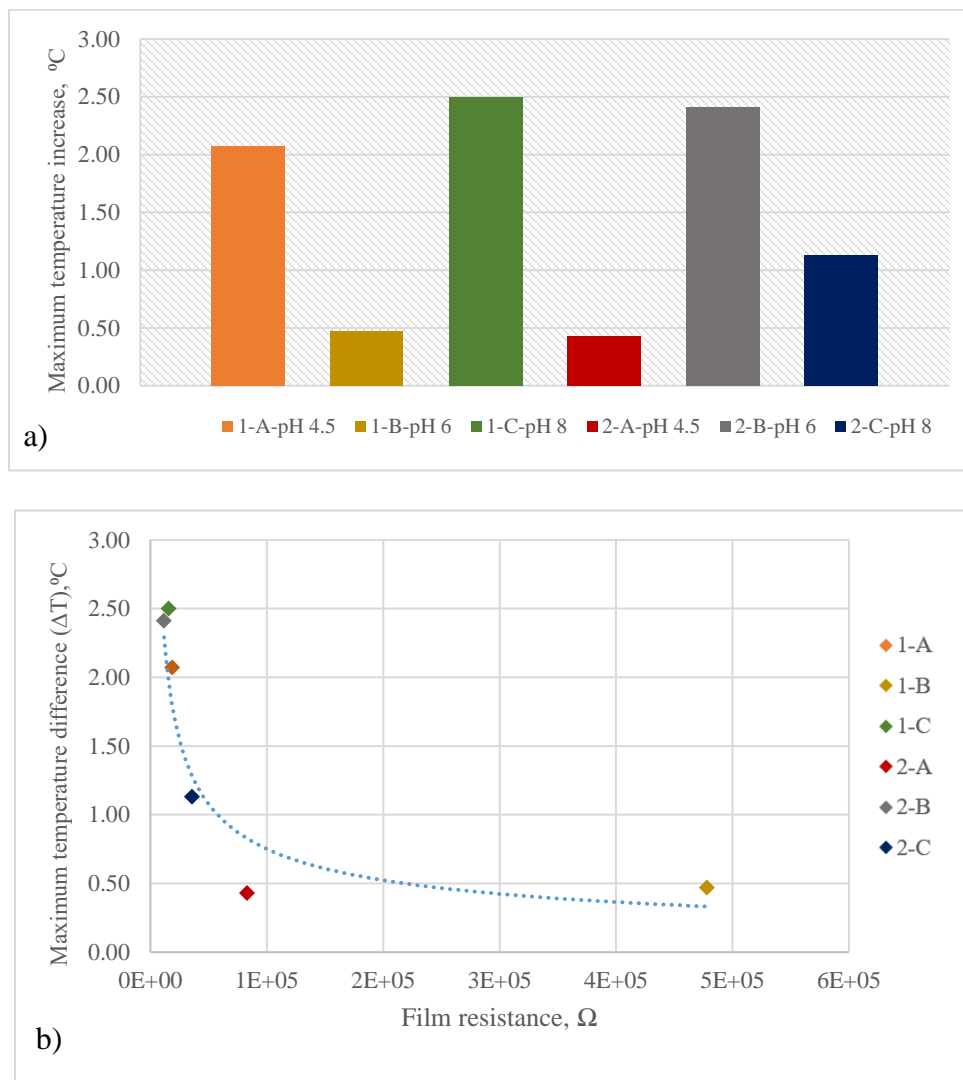


Figure 3.7 a) Maximum temperature increase for samples 1 of experiment 1 and experiment 2, b) Maximum temperature increase dependency on film resistance

Figure 3.8 represents a temperature derivative plot for samples of experiment 1 and 2. It depicts the rise in temperature and steady state temperature regime and the cooling

profile. It could be observed from Figure 3.8 that time for these samples to reach the steady-state temperature regime was about 180 seconds after the application of voltage.

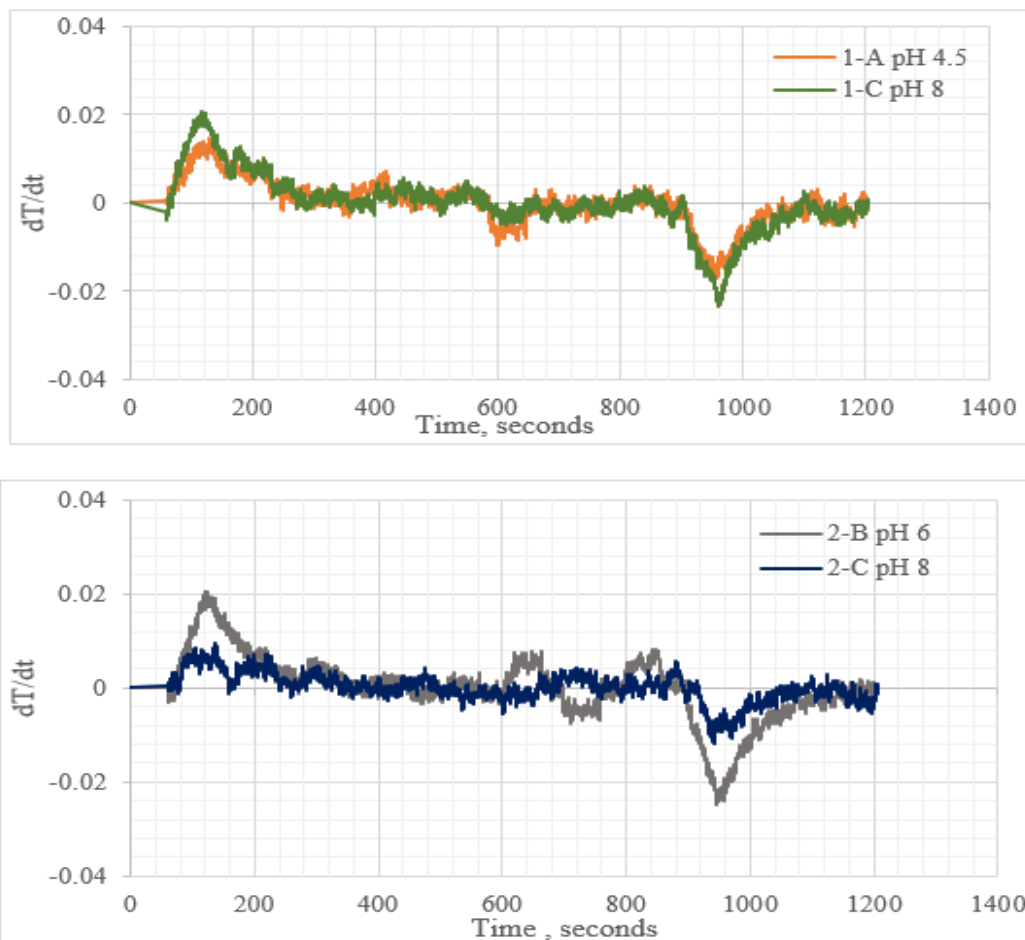


Figure 3.8 Temperature derivative curves for the samples of experiment 1 and 2 plotted over time.

The current (I), voltage (V) characteristics (I-V characteristics), and power characteristics were analyzed for each sample when applied voltage was increased from 0 to 20 V in steps of 2.22 V. From Figure 3.9, there was no change observed in I-V characteristics of the above samples despite applied voltage and temperature rise of the

later. This means that no resistance change is observed despite the fact that CNTs typically exhibit a temperature and voltage dependency.

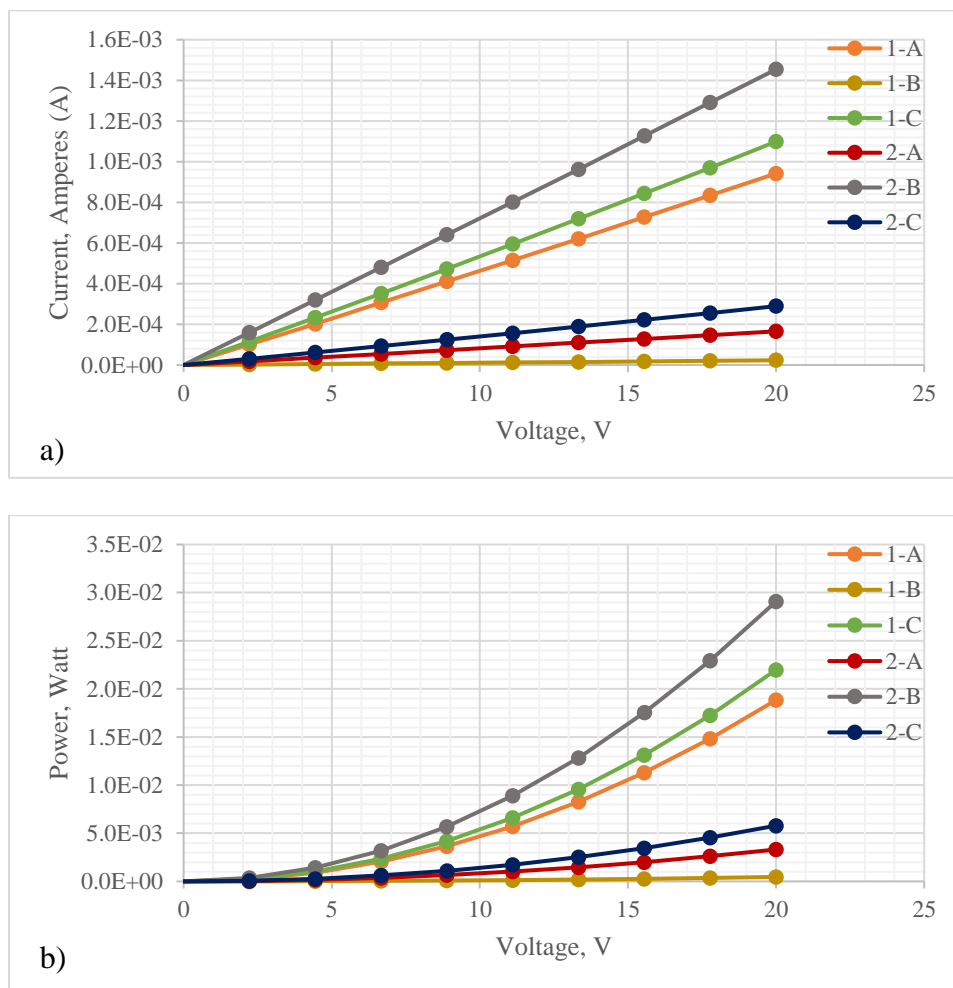


Figure 3.9 Current, voltage and power characteristics of the CNT film heater, a) Change of current for incremental voltage in steps of 5 from 0 to 20 V, b) Power of the heater for incremental voltage in steps of 2.22V from 0 to 20 V.

3.1.2.3. Repeatability Testing

The samples were tested three times to check if they could produce the same temperature distribution across the entire surface. The samples demonstrated a similar

temperature profile and temperature distribution across the surface of the film. The repeated temperature profile for sample 1 of experiment 1 and experiment 2 is given in Figure 3.10. Figure 3.10 (a, b, d, e) shows the same temperature profile when repeated for three trials, while in Figure 3.10 (c, f) there is a 15 to 30% change in the temperature rise.

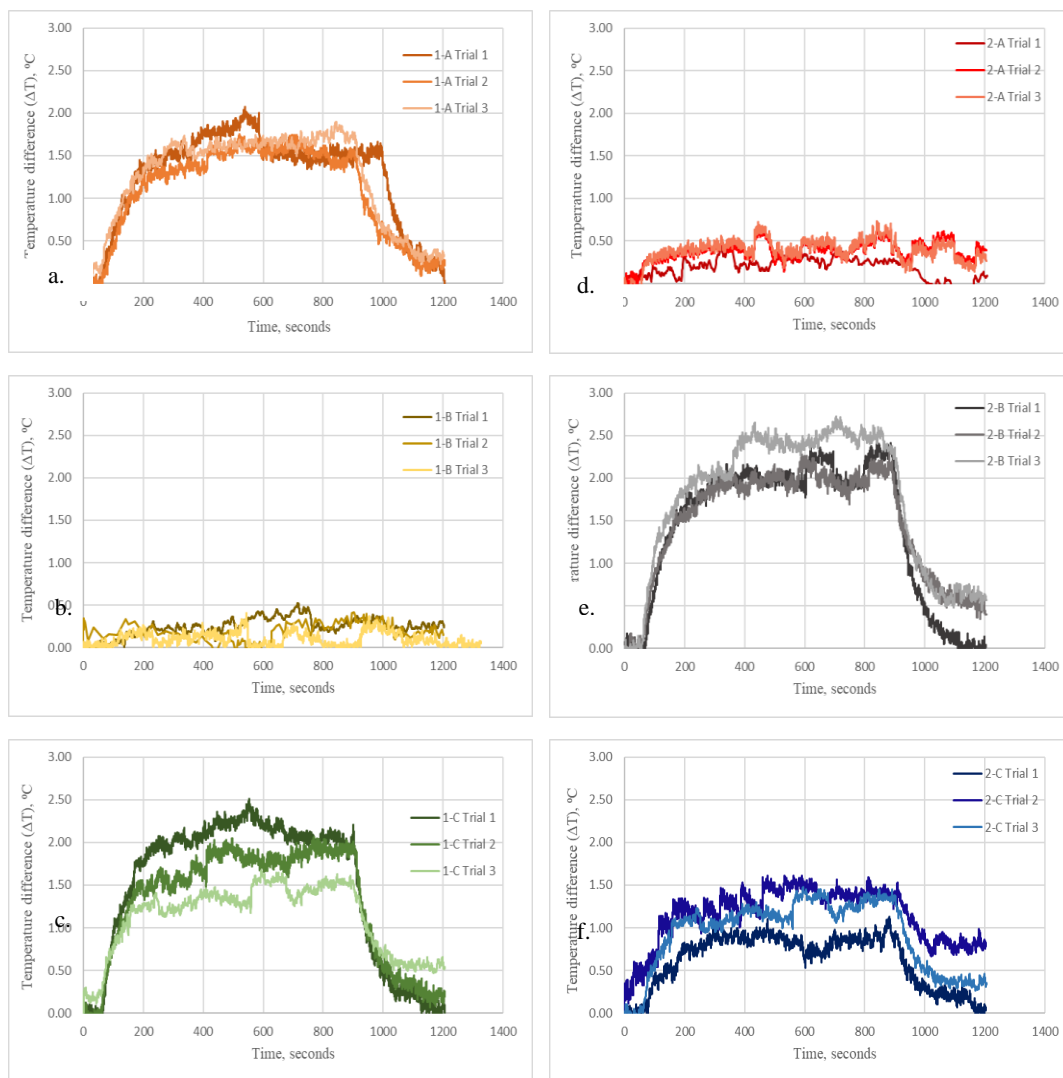


Figure 3.10 Temperature increase profiles for experiments 1 and 2 at an applied voltage of 20 V repeated for 3 trials on the same sample. a) Experiment 1-A, b) Experiment 1-B, c) Experiment 1-C, d) Experiment 2-A, e) Experiment 2-B, f) Experiment 2-C.

3.1.3. Transmittance Testing

The transmittance gives the measure of the amount of light that passes through the sample to the light incident on the sample. The transmittance of light provides information that could be used for many applications. Typical applications include testing window tints of cars, airplanes, and measurements of glass clarity. Here we are studying the transmittance of the prepared film to make sure it is compatible with windshields of cars and aircraft. Until 2017, the federal aviation regulations in Section 23.775 stated that windshield and side windows forward of the pilot's back when the pilot was seated in the normal flight position must have luminous transmittance of no less than 70%. Further, federal motor vehicle standard number 205 (Vandal, 2007) also requires automotive vehicles to have transmittance not less than 70%.

Here we are analyzing the transmittance of the samples for which temperature profile was measured. The transmittance of the samples was measured using the Evolution™ Bio UV-Vis spectrophotometer. The transmittance was studied for visible light wavelength ranging from approximately 380 nm to 740 nm.

3.1.3.1. Transmittance Testing Results

The transmittance was measured for samples of experiment 1 and experiment 2. From Figure 3.11, it was observed that both the experiments exhibited transmittance greater than 50% for the entire region. The experiment set 2 had transmittance values greater than 70% for higher wavelengths from 550 nm to 740 nm.

Sample 1-A had an average transmittance of about 50-60% while sample 1-B and 1-C had a transmittance in the range of 55-65% and 65-70%, respectively. For experiment 2, samples 2-A, 2-B, 2-C demonstrated transmittance ranged between 55 and 75%. The

transmittance values of fabricated film heaters were close to the required transmittance levels of windshields of automobiles and aircraft, however, did not meet the required criterion.

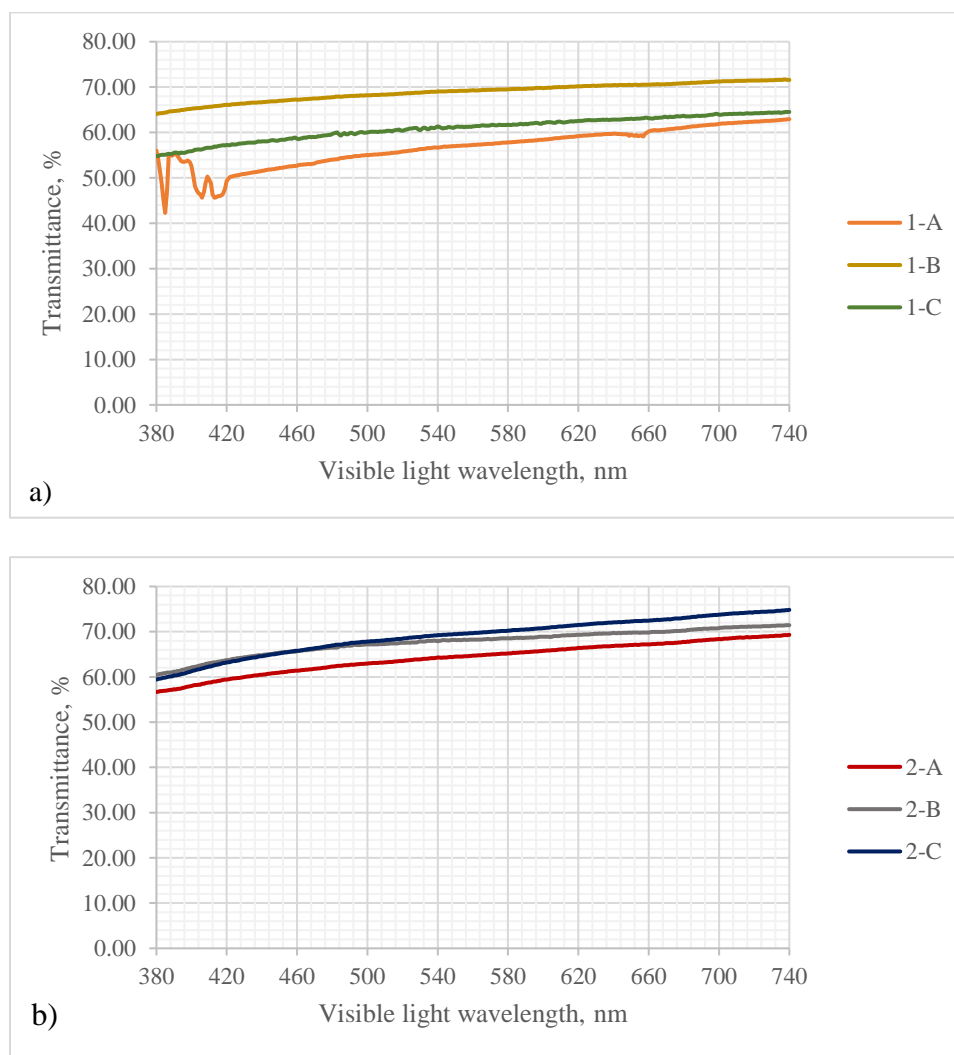


Figure 3.11 Transmittance spectra of fabricated CNT films in the visible light spectra. Transmittance of a) experiment set 1 and b) experiment 2 taken at room temperature.

One factor that hinders the transmittance is the number of layers of CNTs deposited on the substrate. In numerous research studies, it was highlighted that as the number of

layers of CNT layers is increased, the film resistance decreases proportionally. The greater the number of CNTs on the substrate, the conductive percolating network is formed more easily and draws more current at a given voltage. However, with the increase in the number of layers of CNTs, the transmittance of the film heaters will be substantially decreased. Hence improvements have to be made to balance film resistance and transmittance without sacrificing the transparency of the heater.

3.1.4. Sample Characterization

The morphology of the fabricated film heater was characterized by Scanning Electron Microscope (SEM), and the results are shown in Figure 3.12. Currently, the SEM image is obtained for only one sample of experiment 1-C. From the SEM image shown in Figure 3.12, the thin wire-like structures are the carbon nanotubes deposited on one spot on the glass substrate. The image is obtained at 30000x magnification.

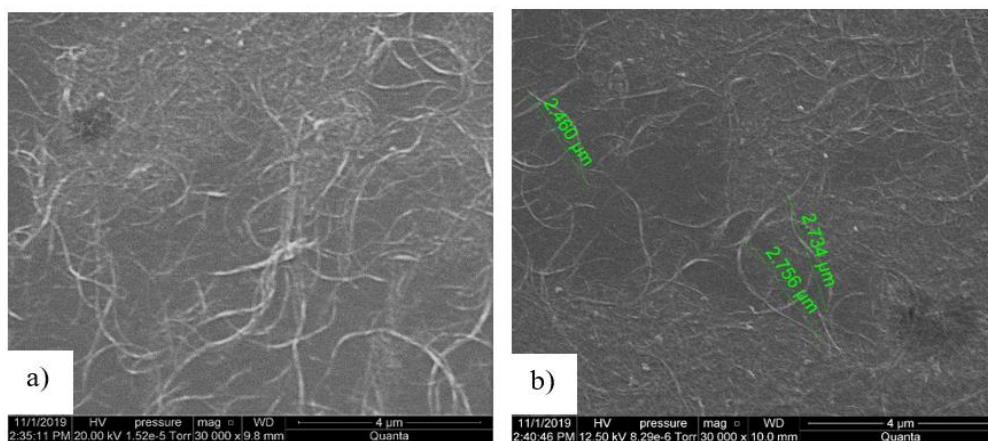


Figure 3.12 SEM image of film heater containing 3 layers of spin coated CNTs taken at different spots. a) Morphology of CNTs deposited on the film at 30000x magnification, b) Length of CNTs measured in SEM at 30000x magnification.

The insets show the schematics of the 2D film heater. It could be seen from the Figure that the SWCNTs are well separated from each other and are not bundled due to van der Waals forces. This verifies that the new approach to the non-covalent functionalization technique introduced in Chapter 2 has resulted in well-dispersed solution of CNTs. Further, there are some vacant spaces between CNT networks and some spaces are filled with more number of CNTs. This means that the spin coating of CNTs on the substrate was not uniform, and these vacant spaces and high concentrations of CNTs in certain other spots will significantly increase the resistance of the film. Also, the average length of CNTs is approximated to be around 3 μm .

3.2. Summary

This chapter details the experiments and tests conducted on the fabricated CNT based film heater. Two sets of experiments were conducted to study the influence of pH and the polyaromatic moiety on the electrothermal characteristics of the CNT network. Further, we analyze the IV characteristics of the CNT network deposited on a thin glass substrate, the thermal response of the CNT film to the applied voltage. A comparison is drawn between experiment set 1 and experiment 2, and samples of different pH. Finally, we discussed the transmittance of the film heater and possible factors that influenced the transmittance of the developed heater.

4. Discussion, Conclusions, and Recommendations

4.1. Discussion

In this work, we have worked on developing a novel technique to enhance the electronic and thermal properties of SWCNTs. Here we have established a unique non-covalent functionalization technique using a combination of super acids and polyaromatic moiety. This method aimed to achieve a homogeneous well-dispersed solution of SWCNTs along with improving the electrical properties of CNTs. Section 3 describes the specific compounds involved, quantities, and solution synthesis procedure to achieve a non-covalent functionalization of SWCNTs.

Using this procedure, we have synthesized a series of experimental solutions by varying the composition of polyaromatic moiety and maintaining different pH at an intermediate step. Further, the resulting solutions were spin-coated and SWCNT based flexible transparent film heaters were fabricated using each of the solutions. Multiple measurements and tests such as the conductivity test, electrothermal test, and transmittance test were performed to observe the electrical characteristics, thermal distribution, and transparency of the film heater. During this testing process, we analyzed that some samples exhibited a relatively high resistance and standard deviation. The nonlinearity in results arose due to several factors such as the increased hours of sonication, impurities on the glass substrate due to environmental surroundings, choice of electrodes and non-uniform distribution of CNTs during the spin coating procedure. Further the samples that resulted in a higher resistance value were made using a new bottle of PBA which had a different lot number and a different purity. Although the manufacturer ensured that PBA was of equal quality, and it might just be coincidental

that all the samples produced with this new lot number had a higher resistance, it might be worth repeating the experiments with a new product.

The samples which depicted lower resistance were quantitatively analyzed for the relationship between temperature change and time in Chapter 3. The time dependent temperature profile shows that film heaters demonstrate an immediate and fast heating and cooling response when a driving voltage of 20V was turned on and off. A temperature increase of 1.5°C to 2.5°C and saturation was achieved within 180 seconds of the applied voltage. This provides a possibility for the film heater to be used in de-icing and defrosting applications. Repeated thermal tests performed on the sample produced a similar temperature profile over the same time and proved that the CNT film heaters show stable electrical and thermal characteristics despite the application of voltage and heat generation on the heater. Hence the electrical and thermal performance results showed that the heaters exhibited chemical stability and could be robust and reliable thin film heaters for various practical applications.

4.2. Conclusions

In conclusion, we have demonstrated detailed research into developing a unique non-covalent functionalization technique that could be used for achieving uniform and homogeneous dispersion of CNTs. We performed two sets of experiments, to study how the increase in polyaromatic moiety affected the overall characteristics of the random network of CNTs in a film. Different pH was maintained during the experiment to analyze if it affected the characteristics of the CNTs and PBA in the solution. However, for solutions to the same experiment with different pH, comparison and analysis could not be made in this research. This was because specific pH was maintained at an

intermediate step while titrating a weak base of ammonium hydroxide into a strongly acidic solution of CNTs, PBA, and fuming sulfuric acid. There were series of dilutions and addition of weak base to each of the solutions to make it environmentally friendly and compatible for practical applications. Also, the amount of weak base influenced each solution differently depending on the amount of PBA in the synthesized solution yielding a salt of a weak acid and a weak base. Hence, these pH values could not be used for a direct comparison of test results. Further, while studying the influence of polyaromatic moiety, we observed that an increase in polyaromatic moiety increased the resistance of the fabricated film. Hence with this approach, the desired resistance value could be achieved by optimizing the amount of polyaromatic compound used for functionalization. Here an increase in 1-pyrene butyric acid is proved to increase the resistance of the CNT film heaters.

Further, the processed solutions were then used to fabricate transparent film heaters that could be used for de-icing and defrosting applications. The fabricated films show fast heating rate and cooling rates and uniform temperature distribution across the sample and are chemically stable. We attribute these properties to the excellent electrical and thermal properties of CNTs and the developed non-covalent functionalization method, which aided in separating the agglomerated CNTs and producing a free-flowing solution. The fabricated films demonstrate an adequate thermal response at a very low power input. These results are promising not only for de-icing or defrosting applications. However, they could be used to replace conventional heaters in applications such as smart windows, heater dining areas, thermal gloves, and also in innovative applications such as solar panels and portable medical sensors.

Overall, this thesis emphasizes a new method to synthesize free-flowing uniformly dispersed solution using a novel carbon nanotube material. Further, the conventional approaches are made to realize transparent film heaters from these processed solutions. Various performance testing and quantitative analysis were detailed to study the behavior of the heater under ambient conditions. Aspects relating to electrical properties and heating performance of the film heaters were discussed, detailing on-resistance values, achieved steady-state temperatures values, and comparison between samples of two experimental sets with different amounts of PBA. Several challenges were involved in the development of transparent film heaters. Some of the challenges faced in this thesis were to develop a transparent film heater of low resistance without compromising the transmittance of the film. A tradeoff between film resistance and transmittance is a common issue in most transparent film heaters developed using carbon nanomaterials. The described new non-covalent functionalization approach and thin-film heaters are commendable heater applications for thermal components, de-icing windshields, and leading edges of aircraft, medical, and several home appliances.

4.3. Recommendations and Future Work

From the tests performed and the results obtained, there is still a lot more improvement needed to enhance the performance of the developed film heater. Issues related to achieving a uniform spin-coated layer on the glass substrate were the most significant concern leading to large errors in the film's resistance and difficulties in quantitative comparisons of results. Further transmittance achieved by the transparent heaters was approximately around 55%-70%, which was relatively low for it to be used for automotive and aircraft applications. One way to achieve good transparency would be

chemical processes or processes like ultrasonication that could break down the CNTs further. However, ultrasonication of the solutions for a long period leads to the depletion of the electronic nature of CNTs. One possible solution to this limitation would change the coating process. Electro spray coating could be a possible non-destructive technique that could be used to create precise and thin nanofilms on the substrate. This approach helps in creating a film of required thickness with uniform distribution of CNTs across the surface. The advantages of electro spray coating are that diameter of solution droplets could be easily controlled by electric charge level, flow rate, the conductivity of the liquid, which results in a flexible droplet dimension from nanometers to micrometers with excellent size uniformity.

Further, a review article of visibly transparent heaters by Gupta (Gupta et al., 2016) discussed that the thermal performance of the heaters was dependent on various factors such as the electrical and thermal conductivities, the specific heat capacity of the active materials, substrate type and its thickness. Further, it was mentioned that the response time of the thermal heater to reach its saturation temperature was much dependent on the substrate material or the protective encapsulation on top of the heater. Here in this thesis, the active material we used was SWCNTs which are proven to have too high electrical and thermal conductivity. The substrate material we used for the fabrication of the heater was a glass film of 2.5 cm x 2.5 cm with 1.1 mm thickness. Hence to achieve a better performance, ultra-thin glass substrates or thermally stable substrate material or conductive material such as mica could be used preferably used to achieve a higher thermal response. Improvements to the thermal performance could also be made using a synergistic approach using metal oxides and carbon nanomaterials. This establishes a

wired network of metal oxides and CNTs, leading to an efficient design and low power transparent heaters.

Efforts are being made in this research towards minimizing the errors caused by the spin coating and ultrasonication process. Further experiments are being conducted to validate how an increase or decrease in the amount of PBA affects the electrical characteristics of the film heaters. Real-world applications of thermal heaters like defogging or de-icing an aircraft window require CNTs to be deposited in large surface areas with solid uniformity and thickness. Hence the development of innovative approaches to coating the CNTs on a relatively large substrate and achieving a uniform thermal distribution over the large area is needed. There exist extensive futuristic applications for both large area and small area thermal heaters. The developed process provides an efficient, environment-friendly, user-friendly, low cost carbon nanotube film heater that consumes low input power and current and achieves a desired thermal response required for de-icing or defrosting small scale applications.

4.4. Summary

Based on the results obtained in Chapter 3, this chapter examines the advantages of the developed new functionalization procedure and fabricated film heater based on CNTs. It describes the reasons behind the statistical errors on the resistance values of the developed heater and provides methods to minimize the standard deviation in test results. Later in this chapter, the recommendations to optimize the heater performance and its scope in innovative applications are discussed.

REFERENCES

- Advani, S. G., & Hsiao, K.-T. (2012). *Manufacturing Techniques for Polymer Matrix Composites (PMCs)*. Elsevier.
- Ajayan, P. M., & Zhou, O. Z. (2001). Applications of Carbon Nanotubes. In M. S. Dresselhaus, G. Dresselhaus, & P. Avouris (Eds.), *Carbon Nanotubes: Synthesis, Structure, Properties, and Applications* (pp. 391–425). Springer.
https://doi.org/10.1007/3-540-39947-X_14
- Algharagholy, L. A. (2019). Defects in Carbon Nanotubes and their Impact on the Electronic Transport Properties. *Journal of Electronic Materials*, 48(4), 2301–2306. <https://doi.org/10.1007/s11664-019-06955-8>
- Al-Sharafi, A. (2019). *Self-Cleaning of Surfaces and Water Droplet Mobility*.
- Amenta, V., & Aschberger, K. (2015). Carbon nanotubes: Potential medical applications and safety concerns. *WIREs Nanomedicine and Nanobiotechnology*, 7(3), 371–386. <https://doi.org/10.1002/wnan.1317>
- Aqel, A., El-Nour, K. M. M. A., Ammar, R. A. A., & Al-Warthan, A. (2012). Carbon nanotubes, science and technology part (I) structure, synthesis and characterisation. *Arabian Journal of Chemistry*, 5(1), 1–23.
<https://doi.org/10.1016/j.arabjc.2010.08.022>
- Behnam, A., Guo, J., & Ural, A. (2007). Effects of nanotube alignment and measurement direction on percolation resistivity in single-walled carbon nanotube films. *Journal of Applied Physics*, 102(4), 044313. <https://doi.org/10.1063/1.2769953>
- Benelmekki, M., & Erbe, A. (2019). Chapter 1—Nanostructured thin films—background, preparation and relation to the technological revolution of the 21st century. In M. Benelmekki & A. Erbe (Eds.), *Frontiers of Nanoscience* (Vol. 14, pp. 1–34). Elsevier. <https://doi.org/10.1016/B978-0-08-102572-7.00001-5>
- Briefing, F. S. (2020, April 27). *Operation ICICLE*. Medium.
<https://medium.com/faa/operation-icicle-97ad0205aea7>
- Castro, N., Pereira, N., Cardoso, V. F., Ribeiro, C., & Lanceros-Mendez, S. (2019). Chapter 2 - Micro- and nanostructured piezoelectric polymers: Fundamentals and application. In M. Benelmekki & A. Erbe (Eds.), *Frontiers of Nanoscience* (Vol. 14, pp. 35–65). Elsevier. <https://doi.org/10.1016/B978-0-08-102572-7.00002-7>
- Cheap Tubes Inc.* (2019, August 9). AZoNano.Com.
<https://www.azonano.com/article.aspx?ArticleID=4842>

- Chien, A.-T., Cho, S., Joshi, Y., & Kumar, S. (2014). Electrical Conductivity and Joule Heating of Polyacrylonitrile/Carbon Nanotube Composite Fibers. *Polymer*, 55. <https://doi.org/10.1016/j.polymer.2014.10.064>
- Choi, T.-Y., Poulidakos, D., Tharian, J., & Sennhauser, U. (2006). Measurement of the thermal conductivity of individual carbon nanotubes by the four-point three-omega method. *Nano Letters*, 6(8), 1589–1593. <https://doi.org/10.1021/nl060331v>
- Costa, P. M. F. J., Gautam, U. K., Bando, Y., & Golberg, D. (2011). Direct imaging of Joule heating dynamics and temperature profiling inside a carbon nanotube interconnect. *Nature Communications*, 2(1), 421. <https://doi.org/10.1038/ncomms1429>
- Duchon, R. (2010, November). *Icing, fatigue, runway incursions and faulty repair—Lciric / Tableau Public*. <https://public.tableau.com/profile/lciric#!/vizhome/Icingfatiguerunwayincursionsandfaultyrepair/Icing>
- Duchon, R. (2014, December 12). *Remedies to Prevent Plane Crashes Languish / News21 – National*. <http://national.news21.com/2010-2/plane-crashes-avoidable-with-safety-measures-ntsb/index.html>
- Eatemadi, A., Daraee, H., Karimkhanloo, H., Kouhi, M., Zarghami, N., Akbarzadeh, A., Abasi, M., Hanifehpour, Y., & Joo, S. W. (2014). Carbon nanotubes: Properties, synthesis, purification, and medical applications. *Nanoscale Research Letters*, 9(1), 393. <https://doi.org/10.1186/1556-276X-9-393>
- Fu, L., & Yu, A. M. (2014). *Carbon nanotubes based thin films: fabrication, characterization and applications*. 22.
- Gogotsi, Y. (2006). *Carbon Nanomaterials* (1st ed.). CRC Press/Taylor & Francis. <https://b-ok.cc/book/461143/9886cb>
- Gupta, R., Rao, K. D. M., Kiruthika, S., & Kulkarni, G. U. (2016). Visibly Transparent Heaters. *ACS Applied Materials & Interfaces*, 8(20), 12559–12575. <https://doi.org/10.1021/acsami.5b11026>
- Han, Z., & Fina, A. (2011). Thermal conductivity of carbon nanotubes and their polymer nanocomposites: A review. *Progress in Polymer Science*, 36(7), 914–944. <https://doi.org/10.1016/j.progpolymsci.2010.11.004>
- Harris, P. J. F., & Harris, P. J. F. (2009). *Carbon Nanotube Science: Synthesis, Properties and Applications*. Cambridge University Press.

- Hirotsu, J., & Ohno, Y. (2019). Carbon Nanotube Thin Films for High-Performance Flexible Electronics Applications. *Topics in Current Chemistry*, 377(1), 3. <https://doi.org/10.1007/s41061-018-0227-y>
- Hone, J. (2002). *Carbon Nanotubes: Thermal Properties*.
- Vandal, R. (2007). *ISTF2007: Windshield Laws*. (2007). <http://mainland.cctt.org/istf2007/laws.asp>
- Jang, M.-H., & Hwang, Y. S. (2018). Effects of functionalized multi-walled carbon nanotubes on toxicity and bioaccumulation of lead in *Daphnia magna*. *PLoS ONE*, 13(3). <https://doi.org/10.1371/journal.pone.0194935>
- Jeon, I.-Y., Chang, D. W., Kumar, N. A., & Baek, J.-B. (2011). Functionalization of Carbon Nanotubes. *Carbon Nanotubes - Polymer Nanocomposites*. <https://doi.org/10.5772/18396>
- Jia, S.-L., Geng, H.-Z., Wang, L., Tian, Y., Xu, C.-X., Shi, P.-P., Gu, Z.-Z., Yuan, X.-S., Jing, L.-C., Guo, Z.-Y., & Kong, J. (2018). Carbon nanotube-based flexible electrothermal film heaters with a high heating rate. *Royal Society Open Science*, 5(6), 172072. <https://doi.org/10.1098/rsos.172072>
- Jorio, A., Dresselhaus, G., & Dresselhaus, M. S. (Eds.). (2008). *Carbon Nanotubes: Advanced Topics in the Synthesis, Structure, Properties and Applications*. Springer-Verlag. <https://doi.org/10.1007/978-3-540-72865-8>
- J. Sisto, T., N. Zakharov, L., M. White, B., & Jasti, R. (2016). Towards pi-extended cycloparaphenylenes as seeds for CNT growth: Investigating strain relieving ring-openings and rearrangements. *Chemical Science*, 7(6), 3681–3688. <https://doi.org/10.1039/C5SC04218F>
- Kang, T. J., Kim, T., Seo, S. M., Park, Y. J., & Kim, Y. H. (2011). Thickness-dependent thermal resistance of a transparent glass heater with a single-walled carbon nanotube coating. *Carbon*, 49(4), 1087–1093. <https://doi.org/10.1016/j.carbon.2010.11.012>
- Karimi, M., Solati, N., Amiri, M., Mirshekari, H., Mohamed, E., Taheri, M., Hashemkhani, M., Saeidi, A., Asghari Estiar, M., Kiani, P., Ghasemi, A., Moosavi, M., Aref, A. R., & Hamblin, M. (2015). Carbon nanotubes part I: Preparation of a novel and versatile drug-delivery vehicle. *Expert Opinion on Drug Delivery*, 12, 1–17. <https://doi.org/10.1517/17425247.2015.1003806>
- Khalid Saeed, I. (2013). Carbon nanotubes-properties and applications: A review. *Carbon Letters*, 14(3), 131–144. <https://doi.org/10.5714/CL.2013.14.3.131>

- Kim, C.-L., Jung, C.-W., Oh, Y.-J., & Kim, D.-E. (2017). A highly flexible transparent conductive electrode based on nanomaterials. *NPG Asia Materials*, 9(10), e438–e438. <https://doi.org/10.1038/am.2017.177>
- Kumar, A., & Nanda, D. (2019). Chapter 3—Methods and fabrication techniques of superhydrophobic surfaces. In S. K. Samal, S. Mohanty, & S. K. Nayak (Eds.), *Superhydrophobic Polymer Coatings* (pp. 43–75). Elsevier. <https://doi.org/10.1016/B978-0-12-816671-0.00004-7>
- Li, H., Liu, J., & Papadakis, R. (2019). Direct measurement of the surface energy of single-walled carbon nanotubes through atomic force microscopy. *Journal of Applied Physics*, 126(6), 065105. <https://doi.org/10.1063/1.5108935>
- Marconnet, A., Panzer, M., & Goodson, K. (2013). Thermal conduction phenomena in carbon nanotubes and related nanostructured materials. *Reviews of Modern Physics*, 85. <https://doi.org/10.1103/RevModPhys.85.1295>
- MarketsandMarkets. (2015). *Aircraft De-Icing Market Worth \$1.30 Billion by 2020*. <https://www.prnewswire.com/news-releases/aircraft-de-icing-market-worth-130-billion-by-2020-499075371.html>
- Meyyappan, M. (2004). *Carbon Nanotubes: Science and Applications*. CRC Press.
- Mishra, A., Bhatt, N., & Bajpai, A. K. (2019). Chapter 12—Nanostructured superhydrophobic coatings for solar panel applications. In P. Nguyen Tri, S. Rtimi, & C. M. Ouellet Plamondon (Eds.), *Nanomaterials-Based Coatings* (pp. 397–424). Elsevier. <https://doi.org/10.1016/B978-0-12-815884-5.00012-0>
- Morishita, T., Matsushita, M., Katagiri, Y., & Fukumori, K. (2010). Noncovalent functionalization of carbon nanotubes with maleimide polymers applicable to high-melting polymer-based composites. *Carbon*, 48(8), 2308–2316. <https://doi.org/10.1016/j.carbon.2010.03.007>
- Pi-Stacking (chemistry). (2020). In *Wikipedia*. [https://en.wikipedia.org/w/index.php?title=Pi-Stacking_\(chemistry\)&oldid=983650205](https://en.wikipedia.org/w/index.php?title=Pi-Stacking_(chemistry)&oldid=983650205)
- Popov, V. N. (2004). Carbon nanotubes: Properties and application. *Materials Science and Engineering: R: Reports*, 43(3), 61–102. <https://doi.org/10.1016/j.mser.2003.10.001>
- Preparation and Properties of Carbon Nanotube-Based Inks*. (2014, December 3). <https://mrs.digitellinc.com/mrs/sessions/26587/view>
- Proctor, J. E., Armada, D. M., & Vijayaraghavan, A. (2017). *An Introduction to Graphene and Carbon Nanotubes*. CRC Press.

- Saifuddin, N., Raziah, A. Z., & Junizah, A. R. (2012, September 17). *Carbon Nanotubes: A Review on Structure and Their Interaction with Proteins* [Review Article]. *Journal of Chemistry*; Hindawi. <https://doi.org/10.1155/2013/676815>
- Schnorr, J. M., & Swager, T. M. (2011). Emerging Applications of Carbon Nanotubes †. *Chemistry of Materials*, 23(3), 646–657. <https://doi.org/10.1021/cm102406h>
- Sinha, N., & Yeow, J. T.-W. (2005). Carbon nanotubes for biomedical applications. *IEEE Transactions on NanoBioscience*, 4(2), 180–195. <https://doi.org/10.1109/TNB.2005.850478>
- Small Diameter SWNTs (HiPco™). (2020). *NanoIntegris*. <http://nanointegris.com/our-products/small-diameter-swnts-hipco/>
- Song, Y., & Youn, J. (2005). Influence of dispersion states of carbon nanotubes on physical properties of epoxy nanocomposites. *Carbon*, 43, 1378–1385. <https://doi.org/10.1016/j.carbon.2005.01.007>
- Wang, Q., & Moriyama, H. (2011). Carbon Nanotube-Based Thin Films: Synthesis and Properties. *Carbon Nanotubes - Synthesis, Characterization, Applications*. <https://doi.org/10.5772/22021>
- What Is Joule Heating? | SimWiki | SimScale Article*. (2020, October 11). SimScale. <https://www.simscale.com/docs/simwiki/heat-transfer-thermal-analysis/what-is-joule-heating/>
- Yao, N., & Lordi, V. (1998). Young's modulus of single-walled carbon nanotubes. *Journal of Applied Physics*, 84(4), 1939–1943. <https://doi.org/10.1063/1.368323>
- Yoon, Y.-H., Song, J.-W., Kim, D., Kim, J., Park, J.-K., Oh, S.-K., & Han, C.-S. (2007). Transparent Film Heater Using Single-Walled Carbon Nanotubes. *Advanced Materials*, 19(23), 4284–4287. <https://doi.org/10.1002/adma.200701173>
- Zuo, L. (2018, January 11). *Carbon Nanotubes: The Future of the Planet's Freshwater – Young Scientists Journal*. <https://ysjournal.com/carbon-nanotubes-the-future-of-the-planets-freshwater/>